Diffusion SLAM: Localising diffusion sources from samples taken by location-unaware mobile sensors

Roxana Alexandru, *Student Member*, IEEE, Thierry Blu, *Fellow*, IEEE and Pier Luigi Dragotti, *Fellow*, IEEE

***Abstract*—We consider diffusion fields induced by multiple localised and instantaneous sources. We assume a mobile sensor samples the field, uniformly along a piecewise linear trajectory, which is unknown. The problem we address is the estimation of the amplitudes and locations of the diffusion sources, as well as of the trajectory of the sensor. We first propose a method for diffusion source localisation and trajectory mapping (D-SLAM) in 2D, where we assume the activation times of the sources are known and the evolution of the diffusion field over time is negligible. The reconstruction method we propose maps the measurements obtained using the mobile sensor to a sequence of generalised field samples. From these generalised samples, we can then retrieve the locations of the sources as well as the trajectory of the sensor (up to a 2D orthogonal geometric transformation). We then relax these assumptions and show that we can perform D-SLAM also in the case of unknown activation times, from samples of a time-varying field, as well as in 3D spaces. Finally, simulation results on both synthetic and real data further validate the proposed framework.**

***Index Terms*—Diffusion equation, finite rate of innovation (FRI), field and trajectory reconstruction, simultaneous localisation and mapping (SLAM), sampling theory.**

I. Introduction

Sampling of spatiotemporal fields is a problem that has been previously considered, both for retrieving sources of a diffusion field [2]–[14], as well as for estimation of the field from samples [15]–[23]. Some of the real-life applications of sampling and reconstruction of physical fields are the localisation of neuronal source activities from electroencephalographic (EEG) signals [24], the retracing of chemical leakages and nuclear leakages [25], [26], as well as environmental monitoring [27], [28] which has experienced renewed interest in recent years due to the rise in wild forest fires and pollution [29].

Several authors have addressed the problem of sampling and reconstructing physical fields that can be modelled using the diffusion equation [3], [5], whilst some other works have considered more general setups where the fields are modelled by constant coefficient linear partial differential equations, e.g. [16]. With the exception of [16], [21], most of the other methods assume the sensors are fixed and at known locations. Sampling physical fields along trajectories using mobile sensors was considered also in [30]–[32], but in these cases the trajectories are known.

In many applications, however, it is not always possible to know the position of the mobile sensor. This may happen for example, for unmanned aerial vehicles (UAVs) such as drones monitoring remote inaccessible areas or for robots scanning an under-water environment [33], where GPS sensors may not accurately work. A research problem of great interest is therefore the estimation of the position of the mobile sensor, without relying on GPS signal, whilst simultaneously monitoring the environment in which it moves. Simultaneous localisation and mapping (SLAM) is a topic which has received significant interest in robotics [34]. The problem is to localise a moving sensor whose position is unknown, whilst jointly creating a map of the surrounding environment. SLAM algorithms have been proposed for a wide range of applications, such as autonomous robots, self-driving cars or virtual reality devices. Most methods rely on information obtained using optical sensors [35], [36], whilst some methods are tailored to acoustic signals [37], [38].

Recently, the problem of simultaneous localisation and mapping has also been studied in [39], [40], in the context of estimation of a static image, using samples from a moving sensor whose location is unknown. The algorithm proposed in [40] achieves reconstruction of both the sampling trajectory (up to a linear transformation and a shift), as well as the 2D image being sampled.

Nevertheless, there are settings in which visual SLAM is not practical, and therefore other sensor modalities are required to capture information of the surrounding environment. For example, many processes governed by the diffusion equation, such as plume sources, biochemical and nuclear leakage and thermal fields, cannot be captured using visual cameras. Instead, these fields are monitored using infrared thermography or odour detection sensors [41], [42]. Given the different modality of the data, existing SLAM methods based on visual or LiDAR data would not be suitable for these real-life applications.

In this paper, we present a method that allows a mobile sensor to move within an environment in order to estimate *sources of diffusion*. We consider a diffusion field induced by multiple instantaneous point-like sources and through the use of the Green's theorem, we are able to convert the field measurements taken along an unknown trajectory into a sequence of generalised field samples. We then use these field samples to perform simultaneous diffusion source localisation and trajectory mapping (D-SLAM) up to a 2D orthogonal transformation, as depicted in Fig. 1. In order to achieve reconstruction, we make the following assumptions. First, we assume that the variation of the diffusion field over time is negligible and that the activation times of the sources are known. In addition, we assume that there are at least two

Some of the work in this paper was, in part, presented at the IEEE International Conference on Acoustics, Speech and Signal Processing (ICASSP), Barcelona, Spain, May 2020 [1].

(a) (b) (c) (d)

Fig. 1: Unmanned aerial vehicles can help determine radiation after incidents in nuclear facilities or during routine monitoring in (a), and localise wild fires in (b) and (c). The problem we consider in this paper is localising the diffusion sources and the trajectory of the mobile sensor from samples along unknown trajectories, as illustrated in (d).

sources and at least three lines in the trajectory, and that the sources and lines are located on a plane. The framework we develop finds an algebraic solution up to an orthogonal transformation from the true source locations and lines. This framework is then extended to the 3D case as well as the case in which the field is time-varying and the activation times of the sources are unknown. We also relate the problem to classical SLAM, by showing how we can estimate a single diffusion source when the trajectory of the mobile sensor is closed (i.e. the sensor returns to the origin point).

This paper is organised as follows. In Section II we introduce the problem of localising multiple instantaneous diffusion sources from field samples taken along a piecewise linear trajectory. Then, in Section III we show that it is possible to retrieve the source locations and amplitudes as well as the sensor trajectory up to an orthogonal transformation, when the field is static and the source activation times are known. Then, in Section IV we develop a generalised D-SLAM algorithm that deals with the case in which the diffusion process is time-varying, the activation times of the sources are unknown, as well as the case in which the samples are corrupted by noise. We also provide experimental results in Section V, which validate the proposed mathematical framework and generalised D-SLAM algorithm on both synthetic and real thermal data. Finally, we present concluding remarks in Section VI.

II. Problem Formulation

Consider the diffusion field induced by an instantaneous source (localised in both space and time), within a two-dimensional region. The diffusion field will diffuse according to the Green's function [43] as follows:

$$f(\mathbf{x},t) = \frac{1}{4\pi\mu(t-\tau_k)} a_k e^{-\frac{||\mathbf{x}-\mathbf{S_k}||^2}{4\mu(t-\tau_k)}} H(t-\tau_k),$$

where:

a_k = amplitude of the diffusion source,
τ_k = activation time of the diffusion source,
$\mathbf{S_k}$ = coordinates of the source in $\mathbb{R}_2$,
$H(t)$ = unit step function,
μ = diffusivity of the medium.

Then, suppose we sample a field induced by K diffusion sources, and take measurements along a trajectory made up of L lines, as illustrated in Fig. 2 for $K = 2$ and $L = 3$. Assume that the measurements are taken at uniform points, with a step size equal to T_s, and that the length of each line is equal to l_j. Let us denote the start point of each line j with $\mathbf{b_j} \in \mathbb{R}_2$, and describe the vector equation of this line as follows:

$$\mathbf{q}_j(s) = \mathbf{b_j} + s(\mathbf{b_{j+1}} - \mathbf{b_j}),$$

where $\mathbf{q}_j(s)$ are points on line j and $s \in [0,1]$. Then, the spatio-temporal measurements along line j, due to K sources with coordinates $\mathbf{S_k}$ are computed as in [3], [43] and given by:

$$f\left(\mathbf{q}_j(s),t\right) = \sum_{k=1}^{K} \frac{1}{4\pi\mu(t-\tau_k)} a_k e^{-\frac{||\mathbf{q}_j(s)-\mathbf{S_k}||^2}{4\mu(t-\tau_k)}} H(t-\tau_k).$$

We now note that we can express $||\mathbf{q}_j(s)-\mathbf{S_k}||^2$ as follows:

$$\begin{aligned} ||\mathbf{q}_j(s) - \mathbf{S_k}||^2 &= ||\mathbf{b_j} - \mathbf{S_k} + s(\mathbf{b_{j+1}} - \mathbf{b_j})||^2 \\ &= ||\mathbf{b_j} - \mathbf{S_k}||^2 + 2s(\mathbf{b_j} - \mathbf{S_k})^T(\mathbf{b_{j+1}} - \mathbf{b_j}) \\ &\quad + s^2||(\mathbf{b_{j+1}} - \mathbf{b_j})||^2 \\ &\overset{(a)}{=} \left(l_j s + \frac{(\mathbf{b_j} - \mathbf{S_k})^T(\mathbf{b_{j+1}} - \mathbf{b_j})}{l_j}\right)^2 \\ &\quad + ||\mathbf{b_j} - \mathbf{S_k}||^2 - \left(\frac{(\mathbf{b_j} - \mathbf{S_k})^T(\mathbf{b_{j+1}} - \mathbf{b_j})}{l_j}\right)^2, \end{aligned} \tag{1}$$

where (a) follows from the fact that the length of segment j is $||(\mathbf{b_{j+1}} - \mathbf{b_j})|| = l_j$.

Let us denote the direction vector of line j with $\mathbf{c_j}$, where:

$$\mathbf{c_j} = \frac{\mathbf{b_{j+1}} - \mathbf{b_j}}{l_j}, \tag{2}$$

such that $\mathbf{c_j}^T\mathbf{c_j} = 1$. Then, the definition in (2) allows us to re-write (1) as:

$$\begin{aligned} ||\mathbf{q}_j(s) - \mathbf{S_k}||^2 &= \left(l_j s + \left(\mathbf{b_j} - \mathbf{S_k}\right)^T \mathbf{c_j}\right)^2 \\ &\quad + ||\mathbf{b_j} - \mathbf{S_k}||^2 - \left(\left(\mathbf{b_j} - \mathbf{S_k}\right)^T \mathbf{c_j}\right)^2. \end{aligned}$$

If we denote $4\mu(t-\tau_k) = C_k(t)$ and assuming $t \geq \tau_k$, the cumulative measurements along line j from all instantaneous sources $k = 1, ..., K$, are given by:

$$\begin{aligned} f\left(\mathbf{q}_j(s),t\right) &:= f_j(s,t) = \sum_{k=1}^{K} \frac{a_k}{\pi C_k(t)} e^{-\frac{||\mathbf{q}_j(s)-\mathbf{S_k}||^2}{C_k(t)}} \\ &= \sum_{k=1}^{K} \frac{a_k}{\pi C_k(t)} e^{-\frac{||\mathbf{b_j}-\mathbf{S_k}||^2 - \left(\left(\mathbf{b_j}-\mathbf{S_k}\right)^T\mathbf{c_j}\right)^2}{C_k(t)}} e^{-\frac{\left(l_j s + \left(\mathbf{b_j}-\mathbf{S_k}\right)^T\mathbf{c_j}\right)^2}{C_k(t)}} \\ &:= \sum_{k=1}^{K} A_{k,j}(t) e^{-\frac{(l_j s - Y_{k,j})^2}{C_k(t)}}, \end{aligned} \tag{3}$$

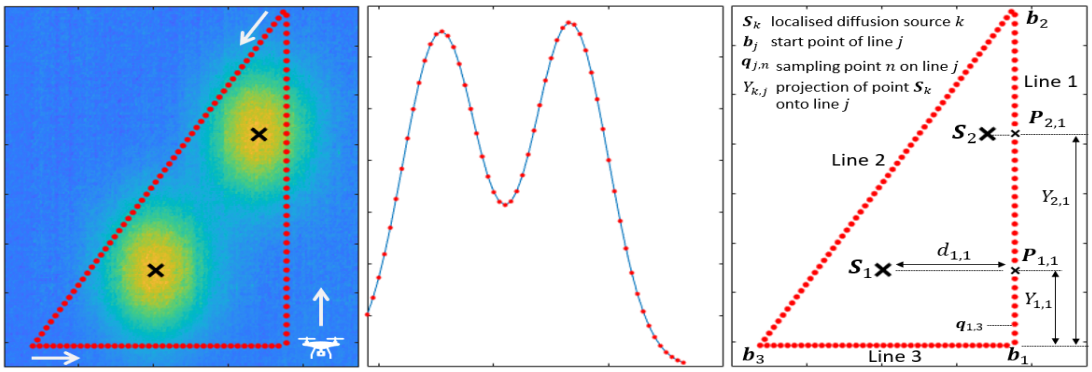

Fig. 2: In (a) we show two thermal sources and the 2D field generated by these sources, sampled by a mobile sensor along a piecewise linear trajectory made of three lines. In (b) we show the projection of the 2D diffusion field across the second line in the trajectory, and the uniform samples taken along this line. The sources are located at $\mathbf{S_1}$ and $\mathbf{S_2}$ respectively, the start point of each line j has coordinates $\mathbf{b_j}$ and the uniformly spaced measurements on line j are denoted with $\mathbf{q_{j,n}}$, as in (c).

where:

$$A_{k,j}(t) = \frac{a_k}{\pi C_k(t)} e^{-\frac{||\mathbf{b_j}-\mathbf{S_k}||^2+Y_{k,j}^2}{C_k(t)}}$$

and

$$Y_{k,j} = \left(\mathbf{S_k} - \mathbf{b_j}\right)^T \mathbf{c_j}. \tag{4}$$

If we assume that within the time interval of observation the evolution in time is negligible, we can remove the dependence on t in $f_j(s,t)$. Moreover, if we assume that the activation time of each source k is known and is the same, we have that $C_k(t) = C$ for some constant C and we set for simplicity $C_k(t) = 1$. Therefore, $f_j(s)$ becomes:

$$f_j(s) = \sum_{k=1}^{K} A_{k,j} e^{-(l_j s - Y_{k,j})^2}.$$

Finally, given that the measurements are taken at uniform points with step size equal to T_s, the reconstruction problem reduces to retrieving the location $\mathbf{S_k}$, the intensity a_k of each source k, and the trajectory from the spatial measurements taken at uniformly spaced locations nT_s, with $n \in \mathbb{N}$:

$$f_j(nT_s) = \sum_{k=1}^{K} A_{k,j} e^{-\left(l_j nT_s - Y_{k,j}\right)^2}, \tag{5}$$

where

$$A_{k,j} = \frac{a_k}{\pi} e^{-||\mathbf{b_j}-\mathbf{S_k}||^2+Y_{k,j}^2}, \tag{6}$$

and

$$Y_{k,j} = \left(\mathbf{b_j} - \mathbf{S_k}\right)^T \mathbf{c_j}, \text{ for } j = 1,..,L \text{ and } k = 1,...,K. \tag{7}$$

Geometrically we note that, when the evolution of the diffusion field over time is negligible, the diffusion field from point-like sources is a sum of 2D Gaussians, as seen in Fig. 2 for the case of two sources. Sampling along straight lines results in a sum of 1D Gaussians, as given in Eq. (5) and shown in Fig. 2 (b). Moreover, the parameters $Y_{k,j}$ in Eq. (7) are the centers of these 1D Gaussians, and also represent the projection of the point $\mathbf{S_k}$ onto line j. This is depicted in Fig. 2 (c), where we see that $Y_{1,1}$ is the projection of $\mathbf{S_1}$ onto the first line. In addition, the parameters $A_{k,j}$ in (6) are dependent on the amplitude a_k of the source and its shortest distance to line j. For example for the case in Fig. 2 (c), we have $A_{1,1} = a_1 e^{-d_{1,1}^2}$.

The problem we consider is the estimation of the unknown parameters $A_{k,j}$ and $Y_{k,j}$, from the measurements given in Eq. (5) along L lines, i.e. for $j = 1, ..., L$. Once the parameters $Y_{k,j}$ and $A_{k,j}$ are estimated, we can then use back-projection to retrieve the source locations $\mathbf{S_k}$ and amplitudes a_k, as well as the lines in the trajectory (determined by the start point $\mathbf{b_j}$ and end point $\mathbf{b_{j+1}}$).

In the following section we present the D-SLAM method for estimation of $K \geq 2$ sources and $L \geq 3$ lines, when the activation time of the sources is the same and is known and the variation of the field during the observation window is negligible. We show that the solution we obtain is unique and up to a 2D orthogonal transformation from the true source locations and trajectory. We then develop a generalised D-SLAM algorithm, by relaxing some of these assumptions and we consider the case in which the field is time-varying, as well as the case in which the activation times of the sources are unknown.

III. D-SLAM using Spatial Samples along Piecewise Linear Trajectories

In this section we present a method for estimating the diffusion field and the trajectory of the sensor in 2D, when the number of sources is $K \geq 2$ and the number of lines $L \geq 3$. We assume that the activation times of the sources are known and equal and that the diffusion field does not evolve over time, such that we have access to the field measurements described in Eq. (5). We also leverage the assumption that the diffusion sources activate before the start of the observation and stay active throughout the observation, such that each source contributes to the measurements on all lines. The trajectory is composed of linear segments located on the same plane as the sources. In addition, all lines whose measurements we use for estimation are adjacent, and their lengths are known. Under these hypotheses, we can state the following result:

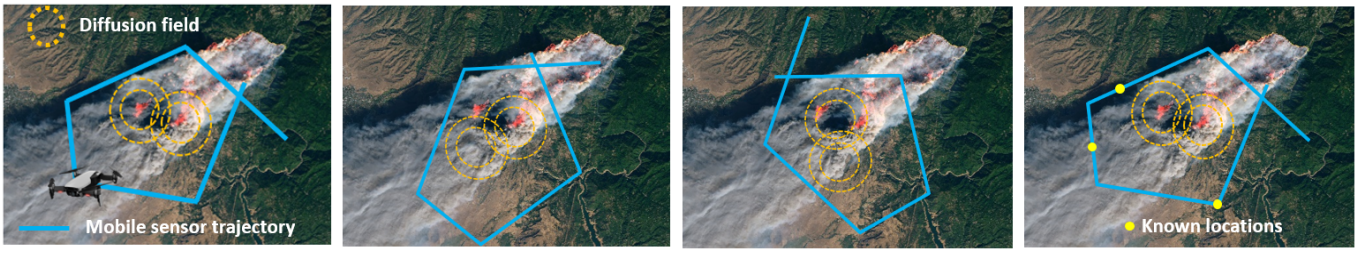

Fig. 3: The problem we consider in this paper is localising the diffusion sources and the trajectory of the mobile sensor from samples along unknown piecewise linear trajectories, as illustrated in (a). Under the hypotheses of Theorem 1, we show that the estimation we obtain is up to a 2D orthogonal transformation (angles and lengths of lines preserved), from the true trajectory and source locations, as seen in the two possible solutions in (b) and (c), provided $K \geq 2$ sources and $L \geq 3$ lines. If the locations of any three points in the trajectory are known, we can exactly retrieve the source locations and the trajectory of the mobile sensor, as seen in (d).

Theorem 1. *Given uniform spatial measurements along an unknown piecewise-linear trajectory, the locations of the sources and the linear segments of the trajectory can be exactly reconstructed up to a 2D orthogonal transformation (shift and rotation), whilst the amplitudes of the sources can be retrieved exactly. For the case in which $K \geq 3$ and $L \geq 3$ or $K = 2$ and $L \geq 4$, the algorithm retrieves a single solution, whereas for $K = 2$ and $L = 3$ there are two solutions, out of which one is up to a 2D orthogonal transformation.*

Proof. In what follows we concentrate on the case $K \geq 3$ and $L \geq 3$. The case $K = 2$ and $L \geq 3$ is discussed in Appendix C. We estimate the trajectory and source locations in the following way. We first estimate the unknown parameters $Y_{k,j}$ and $A_{k,j}$ from the samples $f_j(nT_s)$. We then pair the estimated parameters to the correct source $\mathbf{S_k}$, $k = 1, ..., K$. Finally, given the properly paired parameters, we present an algebraic method to retrieve the sources and the trajectory. As illustrated in Fig. 3, our solution is exact up to an orthogonal transformation.

A. Estimation of $Y_{k,j}$ and $A_{k,j}$

We first need to estimate the parameters $Y_{k,j}$ and $A_{k,j}$ from the measurements in Eq. (5). This is equivalent to a standard estimation problem in the context of finite rate of innovation (FRI) theory [44]. Therefore, these parameters can be retrieved uniquely and exactly using the method in [44] or approximately but more robustly using the approach detailed in Appendix A.

B. Pairing $Y_{k,j}$ and $A_{k,j}$ with $\mathbf{S_k}$

In order to be able to use the estimated parameters $Y_{k,j}$ and $A_{k,j}$ for source localisation, we need to first ensure these are paired across different adjacent lines. In other words, we need to identify whether two parameters $Y_{k,j}$ and $Y_{k',j+1}$ (and the corresponding $A_{k,j}$ and $A_{k',j+1}$ respectively) estimated using measurements on line j and $j+1$ respectively, correspond to the same source $\mathbf{S_k}$, i.e. whether $k = k'$.

First, the parameter $A_{k,j}$ depends on the amplitude a_k of source k, as well as on the shortest distance $d_{k,j}$ from source k to line j, and can also be expressed as:

$$A_{k,j} = a_k e^{-||\mathbf{b_j} - \mathbf{S_k}||^2 + Y_{k,j}^2} \overset{(b)}{=} a_k e^{-d_{k,j}^2}, \tag{8}$$

where (b) follows from Pythagoras' theorem.

Using the derivations in Eq. (8), we get:

$$\log\left(\frac{A_{k,j}}{a_k}\right) = -d_{k,j}^2 = \left(l_j - Y_{k,j}\right)^2 - ||\mathbf{b_{j+1}} - \mathbf{S_k}||^2, \tag{9}$$

where we have used $d_{k,j}^2 + \left(l_j - Y_{k,j}\right)^2 = ||\mathbf{b_{j+1}} - \mathbf{S_k}||^2$ which follows from Pythagoras' theorem, as illustrated in Fig. 4. Here the angle between the vector $\overrightarrow{\mathbf{S_k P_{k,j}}}$ and line j is 90°, which allows us to express $||\mathbf{b_{j+1}} - \mathbf{S_k}||^2$ as the sum of $d_{k,j}^2$ and $\left(l_j - Y_{k,j}\right)^2$.

Similarly, for line $j+1$ and source k', we get:

$$\log\left(\frac{A_{k',j+1}}{a_{k'}}\right) = -d_{k',j+1}^2 = Y_{k',j+1}^2 - ||\mathbf{b_{j+1}} - \mathbf{S_k}'||^2. \tag{10}$$

Eq. (9) and Eq. (10) yield:

$$\log\left(\frac{A_{k,j}}{A_{k',j+1}}\frac{a_{k'}}{a_k}\right) = d_{k',j+1}^2 - d_{k,j}^2$$

$$\overset{(c)}{=} ||\mathbf{S_{k'}} - \mathbf{b_{j+1}}||^2 - Y_{k',j+1}^2 + \left(l_j - Y_{k,j}\right)^2 - ||\mathbf{b_{j+1}} - \mathbf{S_k}||^2, \tag{11}$$

where (c) follows from Pythagoras' theorem.

When $k = k'$, the sources k and k' coincide and have same amplitude a_k, as well as location $\mathbf{S}_k$. If we replace $a_k = a_{k'}$ and $\mathbf{S}_k = \mathbf{S_{k'}}$ into Eq. (11), we get the identity $\log\left(\frac{A_{k,j}}{A_{k',j+1}}\right) = (Y_{k,j} - l_j)^2 - Y_{k',j+1}^2$.

This means that $\log\left(\frac{A_{k,j}}{A_{k',j+1}}\right) = (Y_{k,j} - l_j)^2 - Y_{k',j+1}^2$ whenever $k = k'$. Hence, the two parameters $Y_{k,j}$ and $Y_{h,j+1}$ with corresponding amplitudes $A_{k,j}$ and $A_{h,j+1}$ respectively, are related to the same source k, when $\log\left(\frac{A_{k,j}}{A_{h,j+1}}\right) = (Y_{k,j} - l_j)^2 - Y_{h,j+1}^2$[1].

C. Estimation of the trajectory and source parameters

We are now in a position to find the source amplitudes and locations, as well as the trajectory, that are consistent with the field measurements.

[1]The equality $\log\left(\frac{A_{k,j}}{A_{k',j+1}}\right) = (Y_{k,j} - l_j)^2 - Y_{k',j+1}^2$ may also hold for cases when $k \neq k'$. However, this only happens for degenerate arrangements of the sources with respect to the trajectory, for example when the distances from the source $\mathbf{S_k}$ and $\mathbf{S_{k'}}$ to point $\mathbf{b_{j+1}}$ are equal.

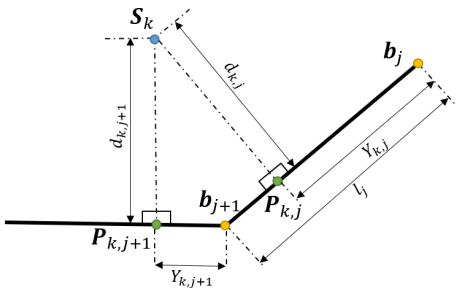

Fig. 4: Single diffusion source and trajectory composed of two lines. The parameter $Y_{k,j}$ is estimated using FRI and represents the projection of the vector $\mathbf{S_k} - \mathbf{b_j}$ onto line j. The point $\mathbf{P_{k,j}}$ is the intersection between the perpendicular from source k to line j, and line j. The shortest distance between the source k and line j is $d_{k,j}$.

Using the parameters $Y_{k,j} = (\mathbf{b_j} - \mathbf{S_k})^T \mathbf{c_j}$ from Eq. (7), we can also obtain the difference $\Omega_{j,q} = Y_{q+1,j} - Y_{q,j} = \left(\mathbf{S_q} - \mathbf{S_{q+1}}\right)^T \mathbf{c_j}$ for each line j and any two different sources q and $q+1$. This leads to the following matrix:

$$\begin{aligned}\mathbf{\Omega} &= \begin{bmatrix} (\mathbf{S}_2 - \mathbf{S_1})^T\mathbf{c_1} & \dots & (\mathbf{S_2} - \mathbf{S_1})^T\mathbf{c}_L \\ (\mathbf{S}_3 - \mathbf{S_2})^T\mathbf{c_1} & \dots & (\mathbf{S_3} - \mathbf{S_2})^T\mathbf{c}_L \\ \vdots & \ddots & \vdots \\ (\mathbf{S_k} - \mathbf{S_{K-1}})^T\mathbf{c_1} & \dots & (\mathbf{S_k} - \mathbf{S_{K-1}})^T\mathbf{c}_L \end{bmatrix} \\ &= \underbrace{\begin{bmatrix} (\mathbf{S_2} - \mathbf{S_1})^T \\ (\mathbf{S_3} - \mathbf{S_2})^T \\ \vdots \\ (\mathbf{S_k} - \mathbf{S_{K-1}})^T \end{bmatrix}}_{(K-1)\times 2} \underbrace{\begin{bmatrix} \mathbf{c_1} & \mathbf{c_2} & \dots & \mathbf{c_L} \end{bmatrix}}_{2\times L} := \mathbf{SC}. \end{aligned} \tag{12}$$

Since we assume the diffusion field is induced within a 2D region, $\mathbf{S}_k$ and $\mathbf{c}_j$ are two-dimensional vectors and hence the dimensions of $\mathbf{S}$ and $\mathbf{C}$ are $(K-1)\times 2$ and $2\times L$ respectively. Therefore, $\mathbf{\Omega}$ is a matrix of $\text{rank} \leq 2$.

We can factorise the matrix $\mathbf{\Omega}$ using singular value decomposition as $\mathbf{\Omega} = \tilde{\mathbf{U}}\tilde{\mathbf{\Delta}}\tilde{\mathbf{V}}^T$, where the first two diagonal entries of $\tilde{\mathbf{\Delta}}$ may be non-zero and the other entries of $\tilde{\mathbf{\Delta}}$ are zero. Therefore, selecting the first two columns of $\tilde{\mathbf{U}}$ and the first two rows of $\tilde{\mathbf{V}}^T$, we can obtain the following factorisation:

$$\mathbf{\Omega} = \mathbf{U}\mathbf{\Delta}\mathbf{V}^T, \tag{13}$$

where:

$\mathbf{U} = (K-1)\times 2$ orthogonal matrix,
$\mathbf{\Delta} = 2\times 2$ diagonal matrix,
$\mathbf{V} = L\times 2$ orthogonal matrix.

Hence, $\mathbf{\Delta}\mathbf{V}^T = \mathbf{U}^T\mathbf{\Omega} = \tilde{\mathbf{C}}$, which we denote as:

$$\mathbf{U}^T\mathbf{\Omega} = \tilde{\mathbf{C}} = \begin{bmatrix} \tilde{\mathbf{c}}_1 & \tilde{\mathbf{c}}_2 & \dots & \tilde{\mathbf{c}}_L \end{bmatrix}.$$

Moreover, denoting the transformation matrix between the estimated direction vectors $\tilde{\mathbf{c}}_\mathbf{j}$ and the true lines $\mathbf{c_j}$ with $\mathbf{A}$, we get:

$$\mathbf{U}^T\mathbf{\Omega} = \begin{bmatrix} \tilde{\mathbf{c}}_1 & \tilde{\mathbf{c}}_2 & \dots & \tilde{\mathbf{c}}_L \end{bmatrix} = \mathbf{A}\begin{bmatrix} \mathbf{c}_1 & \mathbf{c}_2 & \dots & \mathbf{c}_L \end{bmatrix}, \tag{14}$$

or equivalently[2]:

$$\begin{aligned}\begin{bmatrix} \mathbf{c}_1 & \mathbf{c}_2 & \dots & \mathbf{c}_L \end{bmatrix} &= \mathbf{A}^{-1}\begin{bmatrix} \tilde{\mathbf{c}}_1 & \tilde{\mathbf{c}}_2 & \dots & \tilde{\mathbf{c}}_L \end{bmatrix} \\ &= \underbrace{\mathbf{A}^{-1}}_{2\times 2}\mathbf{U}^T\mathbf{\Omega}. \end{aligned} \tag{15}$$

Since $||\mathbf{c_j}|| = 1$ and given that $\mathbf{c_j} = \mathbf{A}^{-1}\tilde{\mathbf{c}}_\mathbf{j}$, we have $1 = \tilde{\mathbf{c}}_\mathbf{j}^T\mathbf{A}^{-T}\mathbf{A}^{-1}\tilde{\mathbf{c}}_\mathbf{j}$, $\forall j$. We then denote

$$\mathbf{A}^{-T}\mathbf{A}^{-1} = \begin{bmatrix} a & b \\ b & c \end{bmatrix},$$

where the unknowns a, b, c can be found by solving the system of L linear equations $1 = \tilde{\mathbf{c}}_\mathbf{j}^T\mathbf{A}^{-T}\mathbf{A}^{-1}\tilde{\mathbf{c}}_\mathbf{j}$, for $j = 1, ..., L$, which has a unique solution provided $L \geq 3$.

Once a, b and c are found, we get $\mathbf{A}^{-1} = \mathbf{R}\sqrt{\begin{bmatrix} a & b \\ b & c \end{bmatrix}}$, where $\mathbf{R}$ is an arbitrary orthogonal matrix. Given $\mathbf{A}^{-1}$, we then find the direction vectors $\mathbf{c_j}$ using Eq. (15). By arbitrarily setting the first point in the trajectory $\mathbf{b_1}$, we then retrieve all the other points $\mathbf{b_j}$ using Eq. (2). Finally, the source locations and amplitudes can be retrieved by solving the system of equations obtained using parameters $Y_{k,j}$ given in Eq. (7) for each source k and lines $j = 1, 2, ..., L$:

$$\begin{bmatrix} \mathbf{c}_1^T \\ \mathbf{c}_2^T \\ \vdots \\ \mathbf{c}_L^T \end{bmatrix}\begin{bmatrix} \mathbf{S_k} \end{bmatrix} = \begin{bmatrix} Y_{k,1} + \mathbf{c}_1^T\mathbf{b}_1 \\ Y_{k,2} + \mathbf{c}_2^T\mathbf{b}_2 \\ \vdots \\ Y_{k,L} + \mathbf{c}_L^T\mathbf{b}_L \end{bmatrix}.$$

Once the locations of the sources have been retrieved, their amplitudes can be computed using the estimated parameters $A_{k,j}$ in (6). Finally, given that $\mathbf{R}$ is an arbitrary orthogonal matrix, the final estimation of the trajectory and source locations will be up to an orthogonal transformation from the true lines and locations respectively. □

Remark 1. *By making additional assumptions, the D-SLAM algorithm can also be extended to the case of a single diffusion source. For instance, by assuming the mobile sensor follows a trajectory composed of three linear segments, and that it returns to the starting point as in classical SLAM, we can localise a single source, whilst jointly estimating the trajectory. This estimation method is described in Appendix D.*

Remark 2. *The D-SLAM framework can also be extended to the case in which the sources and trajectory are located in 3D. In this case, we would need $K \geq 4$ sources and $L \geq 6$ lines to solve the problem using the factorisation in (13), as described in Appendix E.*

Remark 3. *If any three points in the trajectory are known, we can use Procrustes analysis to perfectly estimate the sources and trajectory. Alternatively, the orthogonal transformation can also be specified if we know an axis (e.g. the first line in the trajectory), and an angle (e.g. the angle between the first two lines in the trajectory).*

[2]The inverse $\mathbf{A}^{-1}$ does not exist when matrix $\mathbf{S}$ in (12) loses rank, which may happen for a degenerate arrangement of the sources, for example all sources being located on the same line. When this happens, the matrix $\mathbf{U}^T\mathbf{\Omega}$ in (14) has rank one which means $\mathbf{A}$ also has rank one.

TABLE I: Summary of results for localising diffusion sources from samples taken along unknown trajectories. For each case, we highlight the assumptions made, as well as the nature of the solution obtained.

	Trajectory	Separation of sources	Time evolution of the field	Activation times	Solution
1	Piecewise linear	Overlapping sources	Negligible	Known	Estimation of trajectory and source locations up to an orthogonal transformation. Exact retrieval of the source amplitudes.
2	Piecewise linear	Overlapping sources	Present	Known	Approximate estimation of trajectory and sources up to an orthogonal transformation. Approximate retrieval of the source amplitudes.
3	Piecewise linear	Sufficiently separated sources	Negligible	Unknown	Estimation of trajectory and source locations up to an orthogonal transformation. Exact retrieval of the source amplitudes and their activation times.
4	Parametric	Sufficiently separated sources	Negligible	Known	Estimation of trajectory and source locations up to an orthogonal transformation. Exact retrieval of the amplitudes of the sources [46].
5	Parametric	Sufficiently separated sources	Negligible	Unknown	Estimation of trajectory and source locations up to a scaled orthogonal transformation. Exact retrieval of the source amplitudes and activation times [46].

Remark 4. *The number K of sources may be determined by leveraging the properties of the matrix $\mathbf{S}$, built as in (20) in Appendix B, using $2K+1$ consecutive samples, when we know the maximum number of sources K_{max} and assuming the number of samples on each line satisfies $N \geq 2K_{max}+1$. When there are K sources, this matrix is built using $2K+1$ consecutive samples, and its rank is exactly K [45]. Therefore, for each possible value of $K = 1, ..., K_{max}$, we scan all consecutive groups of $2K+1$ samples, in order to build $\mathbf{S}$, and check whether this matrix has rank K. The smallest retrieved value of K is the number of sources.*

IV. Generalised D-SLAM

In this section we highlight the potential for the real-world implementation of the mathematical framework developed in the previous section. We first relax some of the assumptions leveraged and consider the case in which the diffusion field is time-varying, as well as the case in which the activation times of the sources are unknown. We also address the case in which the sensor moves along an arbitrary unknown parametric trajectory, showing how we can estimate the locations of the sources and the trajectory up to an orthogonal transformation. Finally, we show that the reconstruction of the diffusion sources and the trajectory of the mobile sensor can also be achieved when the spatial measurements are corrupted by noise.

In Table I we present a summary of the different settings we consider, by showing the assumptions made and describing the solution we obtain.

A. Time-varying diffusion field

The method we have presented in the previous section requires the diffusion field to be constant over time, so that the uniformly-spaced measurements we obtain are not time-dependent. We now relax this assumption and consider a time-evolving diffusion process, parameterised by Eq. (3).

Let us denote the time at which the observation starts with t_0 and the temporal sampling period with T. Then, the discrete uniform measurements taken at point $\mathbf{q}_j(nT_s)$ on line j in (3) become:

$$f_{j,n} = f(\mathbf{q}_j(nT_s), nT) = \sum_{k=1}^{K} A_{k,j}(nT) e^{-\frac{\left(l_j nT_s - Y_{k,j}\right)^2}{4\mu\left(nT+t_0-\tau_k\right)}}, \tag{16}$$

where the time t_0 and the activation times τ_k are assumed to be known, and

$$A_{k,j}(nT) = \frac{a_k}{4\pi\mu(nT+t_0-\tau_k)} e^{-\frac{||\mathbf{b_j}-\mathbf{S_k}||^2+Y_{k,j}^2}{4\mu(nT+t_0-\tau_k)}}.$$

We approximate the time-varying field with a constant diffusion field, by setting $nT + t_0 - \tau_k = \hat{t}_j - \tau_k$, where $\hat{t}_j$ is the time at which the middle sample on line j is taken. Then, the field measurements in (16) become equivalent to the ones in (5), and we can estimate the source locations and trajectory as described in Section III.

In Fig. 5 we show the actual time-varying field, which is approximated by a static field as described in this section, in the case in which the diffusion starts at $\tau_1 = 0$s, the first measurement is taken at $t_1 = 0.1$s, the diffusivity of the medium is $\mu = 0.0939\,\mathrm{m}^2$/s and the temporal sampling period is $T = 7.8125 \times 10^{-5}$s.

In Fig. 6 we show the errors between the estimated and the actual parameters $Y_{k,j}$ for the first line of the trajectory in Fig. 10 (a). We observe that the estimation error reduces as the speed of the mobile sensor increases and is negligible for speeds larger than 11m/s.

B. Unknown activation times

We now consider multiple instantaneous sources, with *unknown* activation times τ_k. As we mentioned in Section II, the diffusion fields generated by K instantaneous point-like sources is a sum of K 2-D Gaussians. However, when the activation times are different and unknown, the variances of these Gaussians are different and unknown. Consequently, in this new setting and neglecting the time evolution, the field measured along a straight line is a sum of 1-D Gaussians with different variances. Therefore, the problem is now equivalent to estimating the amplitude, location and variance of the Gaussians.

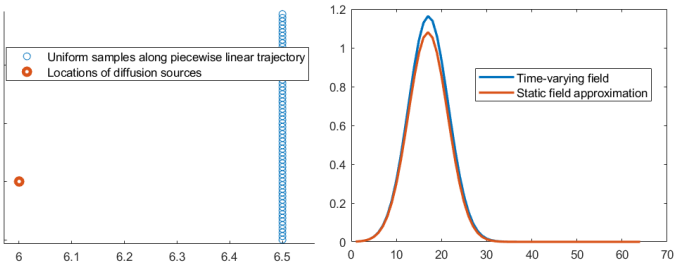

Fig. 5: Time-varying field measurements of a single diffusion source located at distance $d = 0.5$m from a line, when $\mu = 0.0939\,\mathrm{m}^2/s$ and the diffusion starts at $\tau_1 = 0$s, the first measurements is taken at $t_1 = 0.1$s and the temporal sampling period is $T = 7.8125 \times 10^{-5}$s.

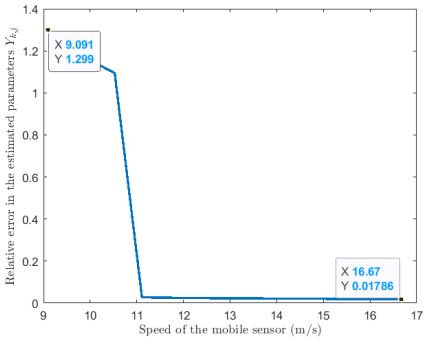

Fig. 6: We consider the setting shown in Fig. 10 (a) and approximate the time-varying field with a static one. We show the relative error of the estimated parameters $Y_{k,j}$ for the first line, for different values of the speed of the mobile sensor, which is computed as $v = \frac{T_s}{T}$.

If the Gaussians are sufficiently separated, we can estimate the parameters of each Gaussian using maximum likelihood estimation, as follows:

First, since we assume the sources are sufficiently separated, groups of samples induced by nearby sources will be separated by samples of small amplitude, $s_n < \epsilon$ where $\epsilon > 0$ and $\epsilon \approx 0$. Therefore, we select the first samples $n = 1, 2, ..., N_1$ such that the next sample has amplitude $s_{N_1+1} < \epsilon$. Using Eq. (3) and assuming the evolution of the diffusion field is negligible, the first N_1 samples are given by:

$$f_1(n) = \frac{a_1}{\pi C_1} e^{-\frac{(l_j n T_s - Y_{1,1})^2}{C_1}},$$

for $n = 1, 2, ..., N_1$, where $C_1 = 4\pi\mu(t_0 - \tau_1)$ with t_0 denoting the start of the observation.

Using maximum likelihood estimation, we can then estimate the parameters of the Gaussian field induced by the first source, using the samples $f_1(n)$. In other words, we can retrieve the optimal amplitude a_1, location $Y_{1,1}$, and variance C_1. Once the unknown parameters are estimated, we retrieve the activation time τ_1 from the variance, using $C_1 = 4\pi\mu(t_0 - \tau_1)$.

We can then find the next group of samples with amplitude $s_n > \epsilon$ in order to retrieve the amplitude a_2, location $Y_{1,2}$ and variance C_2 of the second source. Finally, we repeat these steps in order to estimate the amplitudes and activation times of all sources, as well as the parameters $Y_{k,j}$ for all sources k and lines j. We can then use the method in Section III to retrieve the locations and amplitudes of the diffusion sources, as well as the trajectory.

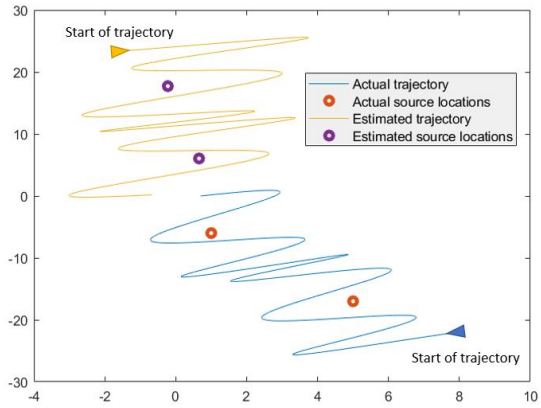

Fig. 7: Actual parametric trajectory and locations of two diffusion sources and estimated trajectory and sources up to an orthogonal transformation, when the activation times of the sources are known.

C. D-SLAM for parametric trajectories

In many real-world applications, the mobile sensor is required to be highly maneuverable, which means that its trajectory cannot be limited to linear segments. Although this assumption was used to derive our algorithm, it is by no means critical as we have shown in [46].

Inspired by the setting in [47], it is possible to consider the following *parametric* trajectory:

$$\mathbf{r}(t) = \sum_{j=1}^{L} \mathbf{c}_j \varphi_j(t),$$

where the multidimensional basis coefficients $\mathbf{c}_j \in \mathbb{R}_2$ are unknown and the functions $\varphi_j(t)$ are known, and as regular as wished.

If the diffusion sources are sufficiently separated and the parametric trajectory is defined using at least two independent basis functions, we can reconstruct the locations of the sources and the parameters of the trajectory up to an orthogonal transformation.

In Fig. 7 we show an example of a parametric trajectory of the mobile sensor and locations of two diffusion sources (taken from [46]), as well as the reconstructed trajectory and source locations, in the case in which the activation times of the sources are known. The estimation is up to an orthogonal transformation from the true parameters.

D. D-SLAM in the presence of noise

The first challenge when the samples are corrupted by noise is the robust estimation of the parameters $Y_{k,j}$ and $A_{k,j}$. One approach to solve the problem is based on the matrix pencil algorithm [48], [49], which was introduced for FRI in [50]. This approach is tailored to the case in which the samples are perturbed by white Gaussian noise. However, in many practical applications this may not be the case, and hence a more robust estimation algorithm such as [51] will be used to denoise the

samples and retrieve the unknowns $Y_{k,j}$ and $A_{k,j}$ for each source k and line j.

Second, given that the retrieved parameters may still not be ideal, the solution found using the estimation method in Section III-C may not always be accurate. To mitigate this problem, once we find the amplitudes and locations of the sources as well as the trajectory using the method in Section III, we refine the estimation as follows.

For each line j, we estimate the perpendicular points from the sources to the lines $\mathbf{P_{k,j}} = \mathbf{b_j} + Y_{k,j}(\mathbf{b_{j+1}} - \mathbf{b_j})$, for $k = 1, ..., K$ (see Fig. 4). Using the estimated source locations, we get the following re-synthesized K field measurements:

$$g(\mathbf{P_{k,j}}) = \sum_{k=1}^{K} \tilde{a}_k e^{-||\mathbf{P_{k,j}} - \mathbf{S_k}||^2}.$$

Suppose that the estimated point $\mathbf{P_{k,j}}$ on line j satisfies $||\mathbf{x_{j,n}} - \mathbf{b_j}|| \leq ||\mathbf{P_{k,j}} - \mathbf{b_j}|| \leq ||\mathbf{x_{j,n+1}} - \mathbf{b_j}||$, where $\mathbf{x_{j,n}} = \mathbf{b_j} + nT_s\left(\mathbf{b_{j+1}} - \mathbf{b_j}\right)$ is the nth measurement point on line j. Then using linear interpolation, we set:

$$\hat{g}(\mathbf{P_{k,j}}) = f(\mathbf{x_{j,n}}) + \left(f(\mathbf{x_{j,n+1}}) - f(\mathbf{x_{j,n}})\right) \frac{||\mathbf{P_{k,j}} - \mathbf{x_{j,n}}||}{||\mathbf{x_{j,n+1}} - \mathbf{x_{j,n}}||},$$

where $f(\mathbf{x_{j,n}})$ is the actual measured field at point $\mathbf{x_{j,n}}$. Hence, we can construct the following system of $LK \times K$ equations (derived from all L lines and K points $\mathbf{P_{k,j}}$ on each line), by imposing $\hat{g}(\mathbf{P_{k,j}}) = g(\mathbf{P_{k,j}})$[3]:

$$\begin{bmatrix} e^{-||\mathbf{P_{1,1}} - \mathbf{S_1}||^2} & \dots & e^{-||\mathbf{P_{K,1}} - \mathbf{S_K}||^2} \\ \vdots & \ddots & \vdots \\ e^{-||\mathbf{P_{K,1}} - \mathbf{S_1}||^2} & \dots & e^{-||\mathbf{P_{K,1}} - \mathbf{S_K}||^2} \\ e^{-||\mathbf{P_{1,2}} - \mathbf{S_1}||^2} & \dots & e^{-||\mathbf{P_{1,2}} - \mathbf{S_K}||^2} \\ \vdots & \ddots & \vdots \\ e^{-||\mathbf{P_{K,2}} - \mathbf{S_1}||^2} & \dots & e^{-||\mathbf{P_{K,2}} - \mathbf{S_K}||^2} \\ \vdots & \ddots & \vdots \\ e^{-||\mathbf{P_{1,L}} - \mathbf{S_1}||^2} & \dots & e^{-||\mathbf{P_{1,L}} - \mathbf{S_K}||^2} \\ \vdots & \ddots & \vdots \\ e^{-||\mathbf{P_{K,L}} - \mathbf{S_1}||^2} & \dots & e^{-||\mathbf{P_{K,L}} - \mathbf{S_K}||^2} \end{bmatrix} \begin{bmatrix} \tilde{a}_1 \\ \vdots \\ \tilde{a}_K \end{bmatrix} = \begin{bmatrix} \hat{g}(\mathbf{P_{1,1}}) \\ \vdots \\ \hat{g}(\mathbf{P_{K,1}}) \\ \hat{g}(\mathbf{P_{1,2}}) \\ \vdots \\ \hat{g}(\mathbf{P_{K,2}}) \\ \vdots \\ \hat{g}(\mathbf{P_{1,L}}) \\ \vdots \\ \hat{g}(\mathbf{P_{K,L}}) \end{bmatrix},$$

which we solve to retrieve the amplitudes $\tilde{a}_k$, for $k = 1, ..., K$.

Once the amplitudes are re-estimated, we can also re-estimate the distance from the source to each line using Eq. (8) as $\tilde{d}_{k,j} = \sqrt{ln(\frac{\tilde{a}_k}{A_{k,j}})}$. Finally, we can use the method in Appendix C-A2 to re-estimate the first two lines in the trajectory based on $\tilde{d}_{k,j}$. This allows us to re-estimate the source locations as in Appendix C-A3, and hence to sequentially re-estimate the remaining trajectory as in Appendix C-A5.

V. Numerical simulations and results

In order to validate the performance of our proposed framework, we perform simulations on both synthetic and real thermal data. In addition, we analyse our approach also for the case of noisy measurements, time-varying fields and unknown activation times. In all cases, once we have estimated the trajectory $\hat{\mathbf{c}}_\mathbf{j}$ and the source locations $\hat{\mathbf{S}}_\mathbf{k}$, $\forall j, k$, we find the orthogonal transformation $\mathbf{Q}$ between the estimated and real lines by solving $\begin{bmatrix}\hat{\mathbf{c}}_\mathbf{1} & \hat{\mathbf{c}}_\mathbf{2}\end{bmatrix}\mathbf{Q} = \begin{bmatrix}\mathbf{c_1} & \mathbf{c_2}\end{bmatrix}$. Once the transformation has been found, we can compute the estimation $\tilde{\mathbf{c}}_\mathbf{j} = \mathbf{Q}^{-1}\hat{\mathbf{c}}_\mathbf{j}$. We validate the performance by comparing the estimated trajectory $\tilde{\mathbf{c}}_\mathbf{j}$ and sources $\tilde{\mathbf{S}}_\mathbf{k}$ with the real values $\mathbf{c_j}$ and $\mathbf{S_k}$ respectively.

A. D-SLAM in the noiseless setting

Fig. 8 shows the estimation results for the retrieval of the 3 lines of a piecewise linear trajectory and 3 diffusion sources, based on the method presented in Section III, when the diffusivity of the medium is $\mu = 1\,\mathrm{m}^2/\mathrm{s}$ and the source amplitudes are all equal to $A = 100$. The estimated locations in Fig. 8 (c) are up to a 2D orthogonal transformation.

The error in the source locations is computed as:

$$E_{sources} = \frac{1}{K}\sum_{k=1}^{K} \frac{||\tilde{\mathbf{S}}_\mathbf{k} - \mathbf{S_k}||_2}{||\mathbf{S_k}||_2},$$

where $\mathbf{S_k}$ is the true location of the source, $\tilde{\mathbf{S}}_\mathbf{k}$ is the estimated location of source k and $||\mathbf{x}||_2$ denotes the L2-norm of $\mathbf{x}$.

The error in the amplitudes E_{amp} is similarly computed and the error of the trajectory is computed as:

$$E_{lines} = \frac{1}{L}\sum_{j=1}^{L}\int_0^1 \frac{||\tilde{\mathbf{r}}_\mathbf{j}(s) - \mathbf{r_j}(s)||_2}{||\mathbf{r_j}(s)||_2} ds,$$

where $\tilde{\mathbf{r}}_\mathbf{j}(s) = \tilde{\mathbf{b}}_\mathbf{j} + l_j\tilde{\mathbf{c}}_\mathbf{j}s$ is the estimated line j and $\mathbf{r_j}(s) = \mathbf{b_j} + l_j\mathbf{c_j}s$ is the true line j.

The error in the estimated source locations is $E_{sources} = 4.6036 \times 10^{-10}$, the error in the estimated amplitudes is $E_{amp} = 3.8365 \times 10^{-9}$ and the error of the lines is $E_{lines} = 9.2052 \times 10^{-10}$, which shows that reconstruction is exact up to numerical precision.

Fig. 9 shows the results of the D-SLAM algorithm, for estimation of the sources and trajectory of the mobile sensor in 3D. This estimation is up to an orthogonal transformation, which is validated by the fact that the resynthesized field measurements are the same as the observed ones.

B. Generalised D-SLAM in the presence of noise

For the case depicted in Fig. 10, we assume the mobile sensor moves along a piecewise linear trajectory, and takes uniform spatio-temporal samples of a time-evolving diffusion field generated by two instantaneous sources, whose activation times are equal and known. The samples are corrupted by additive white Gaussian noise, the diffusivity of the medium is $\mu = 0.0939\,\mathrm{m}^2/\mathrm{s}$ and the temporal sampling period is $T = 1.65 \times 10^{-3}\mathrm{s}$. The samples are denoised using the algorithm in [51], and then we use the method in Section IV-D to perform D-SLAM. The reconstructed trajectory and source locations in (d) as well as the resynthesized field measurements in (e) demonstrate that the D-SLAM algorithm performs well in non-ideal settings.

For the results in Table II we consider the case in which we take measurements of a field generated by K diffusion

[3]A different set of points may be used to construct the system of linear equations. However, it has been empirically observed that using the projection points $\mathbf{P_{k,j}}$ leads to higher accuracy of estimation.

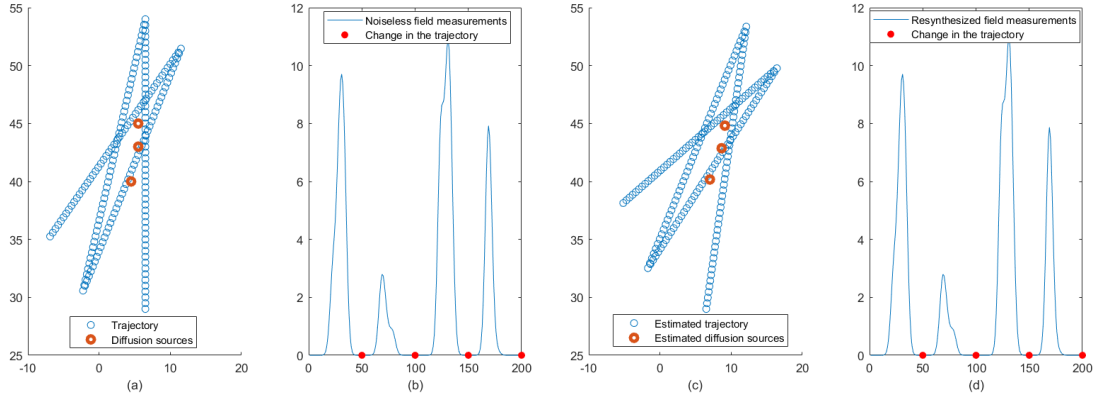

Fig. 8: Three diffusion sources and linear trajectory of three lines in (a), observed measurements along the trajectory in (b), reconstruction of the sources and trajectory up to an orthogonal transformation (rotation and shift) in (c), and resynthesized measurements in (d). The diffusivity is equal to $\mu = 1\,\mathrm{m}^2/\mathrm{s}$ and the start times of the sources are equal and known.

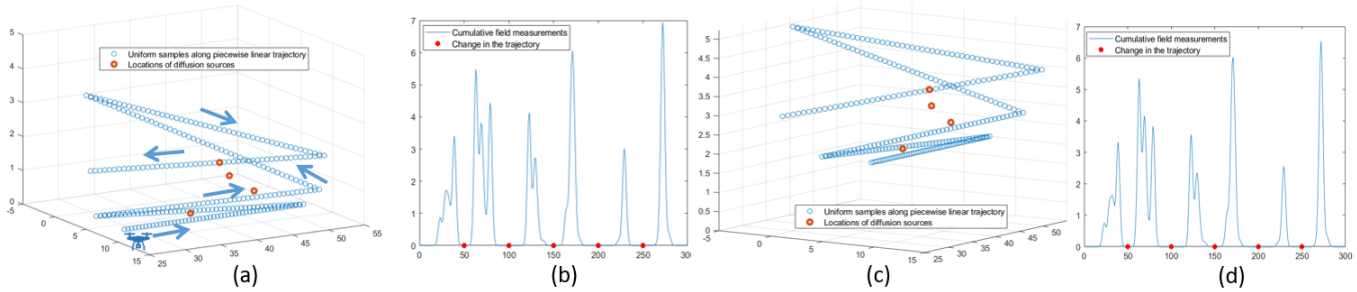

Fig. 9: True source locations and piecewise linear trajectory of the mobile sensor in 3D in (a), observed measurements in (b), estimation up to an orthogonal transformation in (c), and resynthesized measurements along the estimated trajectory in (d). The diffusivity is equal to $\mu = 1\,\mathrm{m}^2/\mathrm{s}$ and the start times of the sources are equal and known.

sources of equal amplitudes $A = 100$, whose activation times are known and equal. The temporal sampling period is denoted with T and a value $T = 0$ means that the field is static, whereas $T \neq 0$ implies a time-varying field. We show errors for the trajectory and locations of the sources, for different values of K and different levels of noise. The results are averaged over 1000 experiments. In Table III we show the reconstruction errors for the case in which the activation times of the sources are unknown. We assume the samples are corrupted by additive white Gaussian noise, and the sources are sufficiently separated as in Fig. 13, which allows us to use the method in Section IV-B to reconstruct the trajectory and source locations. A value $T = 0$ implies that the field is static, as illustrated in Eq. (16) and (5)).

In addition, we use the Cramér-Rao bound to measure the difficulty of estimating the parameters $Y_{k,j}$ from the samples taken on the same line j. This bound allows us to assess the accuracy of the FRI retrieval procedures used in our reconstruction framework, under additive Gaussian noise (see Section III-A). For a comprehensive analysis of the Cramér-Rao bound we refer the reader to [52], [53].

For the setting in Fig. 11, we assume there are $K = 2$ diffusion sources and we use the samples on a single line to estimate $Y_{1,1}$ and $Y_{2,1}$ respectively. The number of samples is $N = 64$, the spatial sampling period is $T_s = 0.0313$m and the diffusivity is equal to $\mu = 0.0939\,\mathrm{m}^2/\mathrm{s}$. We show the average error in the estimated parameters $\Delta Y_{k,1}$ for different distances between the two sources. In Fig. 12, we set the noise level to SNR=20dB and show the estimation errors for different distances between the sources. We can see that the estimation of the parameters is fairly close to the Cramér-Rao bound and that the bound indicates that the estimation is difficult when the distance between the sources is less than 0.3m.

C. D-SLAM for estimation using real thermal data

Next, we evaluate the D-SLAM algorithm for estimation of a single source from real temperature data, obtained by the authors in [3]. A thermal imaging camera has been used to obtain the temperature samples of a diffusion field process in a silicon wafer disc, due to a localised and instantaneous heat source generated by a heat gun [3].

Here we assume a mobile sensor takes uniform samples along an unknown, closed trajectory, such that the start and end points in the trajectory coincide. We first denoise these samples and estimate the parameters $Y_{1,j}$ using the method in [51]. We then leverage the method presented in Appendix D, in order to estimate the location of the source and the lines.

For the results in Fig. 14 we assume the mobile sensor moves at a speed of $v = 0.3292$ m/s (or equivalently 1.18 km/h), and that the temporal sampling period is $T = 0.0027$s. The $N = 180$ uniform measurements from each of the line are plotted in Fig. 14 (a). The results in Fig. 14 (b) show that the source location and the trajectory can be reliably estimated when the activation time of the source is known.

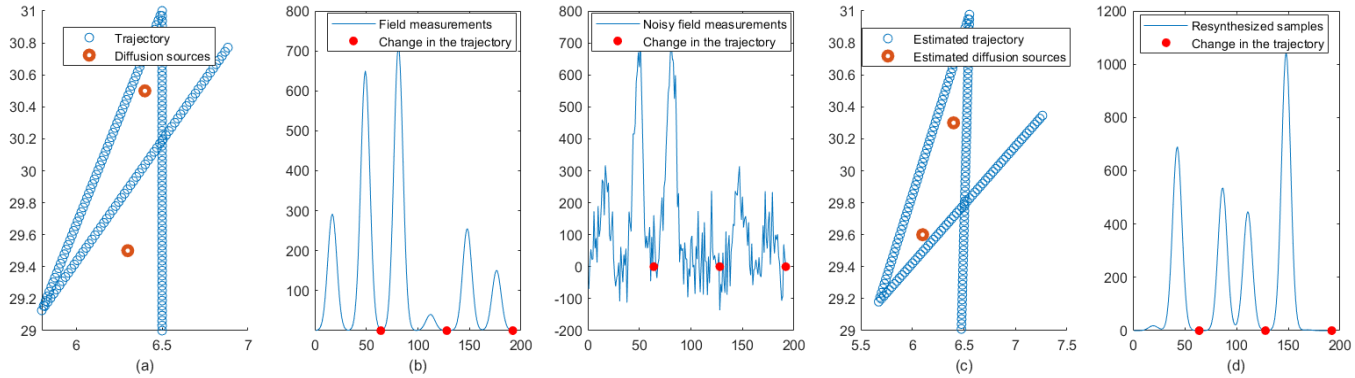

Fig. 10: Estimation of diffusion sources and trajectory of mobile sensor, from noisy spatio-temporal measurements, when SNR=10dB, the activation times of the sources are known and equal, and where the diffusivity is equal to μ =0.0939 m^2/s. The true source locations and trajectory are shown in (a), the noiseless field measurements in (b), the noisy samples in (c), the reconstructed trajectory and source locations when the first line in the trajectory is known in (d), and the resynthesized field measurements in (e).

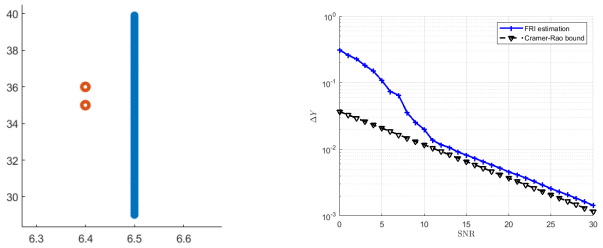

Fig. 11: In (a) we show a setting of two diffusion sources and a single line. In (b) we show the average error and the Cramér-Rao bound for the estimated parameters $Y_{k,1}$ for different levels of noise, when the distance between the two sources is equal to $d = 1$m, as seen in (a).

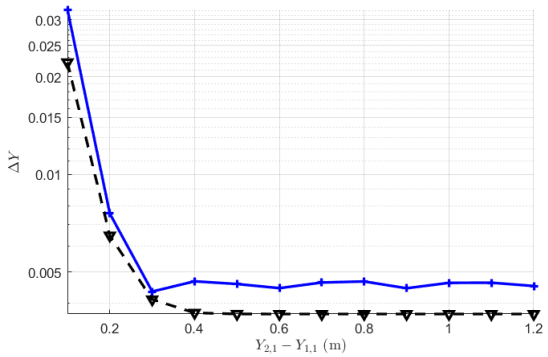

Fig. 12: Average error and the Cramér-Rao bound for the estimated parameters $Y_{k,1}$ for different distances between the two sources, under a 20dB noise corruption.

The distance between the estimated and true source location is $\epsilon = 0.0028$m.

In Fig. 14 (c) we show the estimation of the source location and trajectory, for the case in which the start time is unknown and the temporal sampling period is $T = 1.1 \times 10^{-4}$s. In this case, we use a maximum likelihood estimation method to get an initial estimation for the activation time of the source, and the parameters $Y_{1,j}$ for each line j, as described in Section IV-B. Using the estimated activation time, we then refine the estimation of the unknown parameters $Y_{1,j}$ using the method in [51] and in Appendix D. The distance between the estimated and true source location is $\epsilon = 0.0048$m. The error between the actual start time and the estimated start time is $\epsilon_t = 0.1684$s.

TABLE II: Estimation errors when the sources have the same activation time which is known and the samples are corrupted by additive white Gausian noise. The fields diffused by the sources overlap as in Fig. 10. The spatial sampling period is fixed and equal to $T_s = 0.0313$m, the diffusivity is μ =0.0939 m^2/s and the speed of the mobile sensor is calculated as $v = \frac{T_s}{T}$ for the case in which the field is time-varying.

K	SNR (dB)	T (s)	v (m/s)	$E_{sources}$	E_{lines}
2	30	0	n/a	0.0331	0.0148
2	20	0	n/a	0.0340	0.0132
2	10	0	n/a	0.0373	0.0135
2	5	0	n/a	0.0601	0.0195
2	0	0	n/a	0.0663	0.0188
3	30	0	n/a	0.1561	0.0323
3	20	0	n/a	0.1110	0.0360
3	10	0	n/a	0.1278	0.0375
3	5	0	n/a	0.6613	0.0461
3	0	0	n/a	0.4729	0.0503
3	20	1.65×10^{-2}	1.8969	0.0753	0.0068
3	20	1.65×10^{-3}	18.9696	0.6330	0.0568
3	0	1.65×10^{-2}	1.8969	0.0593	0.0150
2	30	1.65×10^{-2}	1.8969	0.0683	0.0048
2	30	1.65×10^{-3}	18.9696	0.0536	0.0097
2	0	1.65×10^{-2}	1.8969	0.0718	0.0131

VI. Conclusions

In this paper, we have presented a method to estimate multiple instantaneous diffusion sources, from uniform samples taken along unknown piecewise linear trajectories. The source locations, as well as the trajectory can be estimated exactly up to an orthogonal transformation, when we assume we know the activation times of the sources, and that the diffusion field does not evolve over time. The algorithm also achieves accurate

TABLE III: Estimation errors when the field is time varying, the activation times of the sources are unknown and the samples are corrupted by additive white Gausian noise of SNR=30dB. The fields diffused by the sources are sufficiently separated as in Fig. 13.

SNR (dB)	$T(s)$	t_1 (s)	t_2 (s)	$E_{sources}$	E_{lines}	E_{t_1} (s)	E_{t_2} (s)
30	0	1	1	0.0876	0.1195	0.0233	0.0023
30	1.67×10^{-4}	1	1	0.0885	0.1156	0.0247	0.0024
30	1.67×10^{-3}	1	1	0.0397	0.1105	0.0325	0.0110
30	1.67×10^{-4}	1	1.3	0.0267	0.0982	0.1166	0.0157
20	1.67×10^{-4}	1	1.3	0.5454	0.1465	0.3841	0.3412

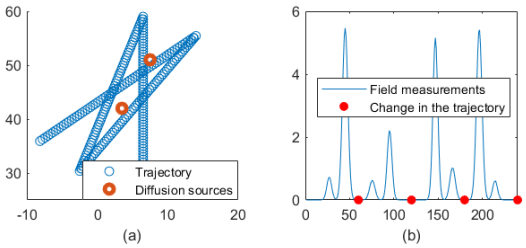

Fig. 13: Two diffusion sources with unknown activation times and trajectory composed of four lines.

estimation when we relax these assumptions. Experimental results on both synthetic and real data show the potential of the proposed algorithm.

Appendix A
Estimating the centers of Gaussian functions from their sum

Leveraging the results in [44], we can multiply the measurements $f_{j,n}$ by the coefficients $c_n = e^{-(l_j nT)^2}$, to obtain the *signal moments* of the form $s_n = \sum_{k=1}^{K} \left(A_{k,j} e^{-(Y_{k,j})^2} \right) e^{2l_j nTY_{k,j}} := \sum_{k=1}^{K} b_k u_k^n$. We then use the annihilating filter method, also known as Prony's method [54] on s_n, to obtain the frequency components u_k, as well as the amplitudes b_k, for $k = 1, ..., K$, provided $N \geq 2K$. This is detailed in Appendix B.

An alternative method is to approximately retrieves the unknown frequencies and amplitudes, which in many cases proves to be more stable and robust to noise.

Using the results in [53], [55], we can find coefficients $c_{m,n}$ that allow us to approximately reproduce exponentials, as follows:

$$\sum_{n \in \mathbb{N}} c_{m,n} e^{-(t-nT)^2} \approx e^{j\omega_m t}, \tag{17}$$

for $\omega_m = \omega_0(1 - \frac{2}{2K-1}m)$, $m = 0, 1, ..., 2K-1$, where K is the number of sources we aim to estimate and ω_0 is arbitrary.

Then, we can multiply the measurements $f_{j,n}$ by the coefficients $c_{m,n}$, to obtain the *signal moments*:

$$\begin{aligned} s_m &= \sum_n c_{m,n} f_{j,n} = \sum_n c_{m,n} \sum_{k=1}^{K} A_{k,j} e^{-(l_j nT - Y_{k,j})^2} \\ &= \sum_{k=1}^{K} A_{k,j} \sum_n c_{m,n} e^{-(l_j nT - Y_{k,j})^2} \overset{(a)}{\approx} \sum_{k=1}^{K} A_{k,j} e^{j\omega_m Y_{k,j}}, \end{aligned}$$

where (a) follows from Eq. (17).

We then use Prony's method [54] on s_m, to obtain the frequency components $Y_{k,j}$, as well as the terms $A_{k,j}$, for each line j and source $\mathbf{S_k}$.

Appendix B
Prony's method

One can retrieve the unknown parameters $\{b_k, u_k\}_{k=1}^K$ from the sequence $s_n = \sum_{k=1}^K b_k u_k^n$ using the annihilating filter method, also known as Prony's method [54]. Let h_n be a filter with zeros at $\{u_k\}_{k=1}^K$, such that when we filter the sequence s_n with this filter, the result will be zero.

The z-transform of this annihilating filter is given by:

$$H(z) = \sum_{n=0}^{K} h_n z^{-n} = \prod_{k=1}^{K} (1 - u_k z^{-1}), \tag{18}$$

which evaluates to zero when $z = u_k$, and whose coefficients h_n can be convolved with the sequence s_n, to obtain:

$$h_n * s_n = \sum_{l=0}^{K} h_l s_{n-l} = \sum_{k=1}^{K} b_k u_k^n \sum_{l=0}^{K} h_l u_k^{-l} \overset{(a)}{=} 0, \tag{19}$$

where (a) holds since $z = u_k$ is a zero of $H(z)$ in Eq. (18).

The filter coefficients h_n can be uniquely retrieved by involving at least $2K$ consecutive values of the signal moments s_n, in order to form K distinct equations as in (19). These can be written in a Toeplitz matrix form, as follows:

$$\begin{bmatrix} s_K & s_{K-1} & \cdots & s_0 \\ s_{K+1} & s_K & \cdots & s_1 \\ \vdots & \vdots & \ddots & \vdots \\ s_{2K-1} & s_{2K-2} & \cdots & s_{K-1} \end{bmatrix} \begin{bmatrix} 1 \\ h_1 \\ \vdots \\ h_K \end{bmatrix} = \mathbf{Sh} = 0. \tag{20}$$

If $\{b_k\}_{k=1}^K$ are non-zero and $\{u_k\}_{k=1}^K$ are distinct, matrix $\mathbf{S} \in \mathbb{C}^{K \times (K+1)}$ has full row rank K, which means the solution $\mathbf{h}$ given by the system in (20) is unique. This solution can be found using the singular value decomposition of $\mathbf{S}$, where $\mathbf{h}$ is the singular vector corresponding to the zero singular value.

Once the filter coefficients h_n of the polynomial $H(z)$ have been found, the parameters $\{u_k\}_{k=1}^K$ are obtained from the roots of this filter, and the parameters $\{b_k\}_{k=1}^K$ can be computed from the linear system of K equations given by $s_n = \sum_{k=1}^K b_k u_k^n$, for $n = 0, 1, ..., K-1$.

Appendix C
D-SLAM when $K = 2$ and $L \geq 3$

We present a method for simultaneous estimation of the locations of the sources, relative to the lines. In particular, this method retrieves the shortest distances $d_{k,j}$ between all sources k and lines j. Using the knowledge of the shortest distances, we can then estimate the trajectory and location of the sources up to an orthogonal transformation.

A. D-SLAM when $L \geq 4$

We first consider the case in which the number of lines satisfies $L \geq 4$, and show that we can uniquely estimate the shortest distances between the sources and the lines. For

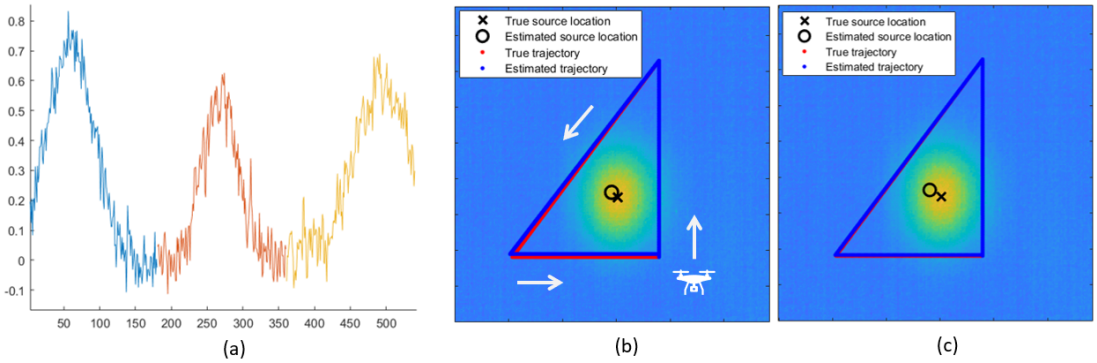

Fig. 14: In (a) we plot the measurements observed along each line in the trajectory (blue for the first line, red for the second, and yellow for the third line respectively). In (b) we display the estimation of a single diffusion source from samples of a real thermal diffusion field, taken along a trajectory of three lines, where the first line is known and when the activation time of the source is assumed to be known. The mobile sensor's speed is $v = 0.3292$ m/s, and the temporal sampling period is $T = 2.7 \times 10^{-3}$s. In (c) we show the reconstruction results for the case in which the activation time of the source is unknown, and the temporal sampling period is $T = 1.1 \times 10^{-4}$s.

simplicity, let us first assume that the number of sources is $K = 2$, and consider the parameters $Y_{k,j}$ in Eq. (6), estimated for three lines $j-1$, j and $j+1$, depicted in Fig. 15.

1) Simultaneous source localisation relative to all lines

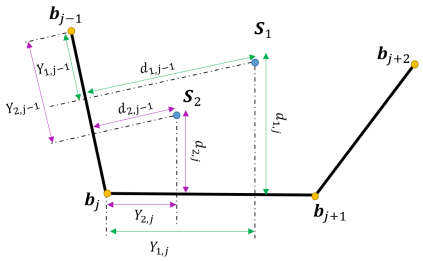

Fig. 15: Two diffusion sources located at $\mathbf{S_1}$ and $\mathbf{S_2}$ respectively, and trajectory made of three lines.

We denote with $\tilde{\mathbf{c}}_\mathbf{j}$ the unit vector orthogonal to $\mathbf{c_j}$ in the couterclockwise direction, and we have that $\tilde{\mathbf{c}}_\mathbf{j}^T \tilde{\mathbf{c}}_\mathbf{j} = 1$.

The location of the source k relative to line j can be computed as $\mathbf{S_k} = \mathbf{b_j} + Y_{k,j}\mathbf{c_j} + d_{k,j}\tilde{\mathbf{c}}_\mathbf{j}$, where $d_{k,j}$ is the shortest distance from the source to line j (see Fig. 15). Similarly, for line $j-1$ we have that $\mathbf{S_k} = \mathbf{b_{j-1}} + Y_{k,j-1}\mathbf{c_{j-1}} + d_{k,j-1}\tilde{\mathbf{c}}_\mathbf{j-1}$. Equating the two expressions and hence eliminating $\mathbf{S_k}$ leads to the following equality for $k \in \{1,2\}$:

$$Y_{k,j-1}\mathbf{c_{j-1}} - \left(\mathbf{b_j} - \mathbf{b_{j-1}}\right) + d_{k,j-1}\tilde{\mathbf{c}}_\mathbf{j-1} = Y_{k,j}\mathbf{c_j} + d_{k,j}\tilde{\mathbf{c}}_\mathbf{j},$$

which, given $\mathbf{c_{j-1}} = \frac{\mathbf{b_j} - \mathbf{b_{j-1}}}{l_{j-1}}$, can be re-written as:

$$\left(Y_{k,j-1} - l_{j-1}\right)\mathbf{c_{j-1}} + d_{k,j-1}\tilde{\mathbf{c}}_\mathbf{j-1} = Y_{k,j}\mathbf{c_j} + d_{k,j}\tilde{\mathbf{c}}_\mathbf{j}. \quad (21)$$

We can express Eq. (21) algebraically as follows:

$$\underbrace{\begin{bmatrix} Y_{1,j-1} - l_{j-1} & d_{1,j-1} \\ Y_{2,j-1} - l_{j-1} & d_{2,j-1} \end{bmatrix}}_{\mathbf{A_{j-1}}} \underbrace{\begin{bmatrix} \mathbf{c_{j-1}} & \tilde{\mathbf{c}}_\mathbf{j-1} \end{bmatrix}^T}_{\mathbf{\Omega_{j-1}}} = \underbrace{\begin{bmatrix} Y_{1,j} & d_{1,j} \\ Y_{2,j} & d_{2,j} \end{bmatrix}}_{\mathbf{A_j}} \underbrace{\begin{bmatrix} \mathbf{c_j} & \tilde{\mathbf{c}}_\mathbf{j} \end{bmatrix}^T}_{\mathbf{\Omega_j}}. \quad (22)$$

Given the counterclockwise orientation of $\tilde{\mathbf{c}}_\mathbf{j}$ relative to line $\mathbf{c_j}$, we have that $\det\left(\mathbf{\Omega_j}\right) = 1$, $\forall j$. Since $\det\left(\mathbf{\Omega_j}\right) = \det\left(\mathbf{\Omega_{j-1}}\right) = 1$, from Eq. (22) we have that:

$$\det\left(\mathbf{A_{j-1}}\right) = \det\left(\mathbf{A_j}\right),$$

or equivalently:

$$\begin{aligned} d_{2,j-1}\left(Y_{1,j-1} - l_{j-1}\right) - d_{1,j-1}\left(Y_{2,j-1} - l_{j-1}\right) \\ = Y_{1,j}d_{2,j} - Y_{2,j}d_{1,j}. \end{aligned} \quad (23)$$

Moreover, squaring both sides of (23), we get:

$$\begin{aligned} & d_{1,j-1}^2\left(Y_{2,j-1} - l_{j-1}\right)^2 + d_{2,j-1}^2\left(Y_{1,j-1} - l_{j-1}\right)^2 \\ & - 2d_{1,j-1}d_{2,j-1}\left(Y_{2,j-1} - l_{j-1}\right)\left(Y_{1,j-1} - l_{j-1}\right) \\ & = d_{1,j}^2 Y_{2,j}^2 + d_{2,j}^2 Y_{1,j}^2 - 2d_{1,j}d_{2,j}Y_{1,j}Y_{2,j}. \end{aligned} \quad (24)$$

Since $\tilde{\mathbf{c}}_\mathbf{j}$ and $\mathbf{c_j}$ are orthonormal vectors, we have that $\mathbf{\Omega}_j^T\mathbf{\Omega}_j = \mathbf{I}$, $\forall j$, where $\mathbf{\Omega}_j$ is defined in (22). Using (22) we then have that $\mathbf{A}_{j-1}\mathbf{\Omega}_{j-1}^T\mathbf{\Omega}_{j-1}\mathbf{A}_{j-1}^T = \mathbf{A}_j\mathbf{\Omega}_j^T\mathbf{\Omega}_j\mathbf{A}_j^T$, and therefore $\mathbf{A}_{j-1}\mathbf{A}_{j-1}^T = \mathbf{A}_j\mathbf{A}_j^T$. This leads to the following three equations:

$$\left(Y_{k,j-1} - l_{j-1}\right)^2 + d_{k,j-1}^2 = Y_{k,j}^2 + d_{k,j}^2, \text{ for } k \in \{1,2\}, \quad (25)$$

and

$$\begin{aligned} \left(Y_{1,j-1} - l_{j-1}\right)\left(Y_{2,j-1} - l_{j-1}\right) + d_{1,j-1}d_{2,j-1} \\ = Y_{1,j}Y_{2,j} + d_{1,j}d_{2,j}. \end{aligned} \quad (26)$$

Denoting

$$\begin{cases} \alpha_j &= \left(Y_{1,j-1} - l_{j-1}\right)^2 - Y_{1,j}^2 \\ \beta_j &= \left(Y_{2,j-1} - l_{j-1}\right)^2 - Y_{2,j}^2 \\ \gamma_j &= \left(Y_{1,j-1} - l_{j-1}\right)\left(Y_{2,j-1} - l_{j-1}\right) - Y_{1,j}Y_{2,j}, \end{cases} \quad (27)$$

we can then use Eq. (25) and (26) to find:

$$\begin{cases} d_{1,j}^2 &= d_{1,1}^2 + \sum_{k=2}^j \alpha_k := d_{1,1}^2 + a_j \\ d_{2,j}^2 &= d_{2,1}^2 + \sum_{k=2}^j \beta_k := d_{2,1}^2 + b_j \\ d_{1,j}d_{2,j} &= d_{1,1}d_{2,1} + \sum_{k=2}^j \gamma_k := d_{1,1}d_{2,1} + c_j, \end{cases} \quad (28)$$

where $a_j = \sum_{k=2}^j \alpha_k$, $b_j = \sum_{k=2}^j \beta_k$ and $c_j = \sum_{k=2}^j \gamma_k$.

We can then replace the expressions in (28) for $d_{1,j}^2$, $d_{2,j}^2$

and $d_{1,j}d_{2,j}$, into Eq. (24) to get:

$$\begin{aligned}
&d_{1,1}^2\left(\left(Y_{2,j-1}-l_{j-1}\right)^2-Y_{2,j}^2\right)+d_{2,1}^2\left(\left(Y_{1,j-1}-l_{j-1}\right)^2-Y_{1,j}^2\right)\\
&-2d_{1,1}d_{2,1}\left(\left(Y_{2,j-1}-l_{j-1}\right)\left(Y_{1,j-1}-l_{j-1}\right)-Y_{1,j}Y_{2,j}\right)\\
&+a_{j-1}\left(Y_{2,j-1}-l_{j-1}\right)^2-a_jY_{2,j}^2+b_{j-1}\left(Y_{1,j-1}-l_{j-1}\right)^2\\
&-b_jY_{1,j}^2-2c_{j-1}\left(Y_{2,j-1}-l_{j-1}\right)\left(Y_{1,j-1}-l_{j-1}\right)\\
&+2c_jY_{1,j}Y_{2,j}=0.
\end{aligned} \tag{29}$$

Leveraging Eq. (27) and (28), we can express (29) in matrix form for $j=2,...,L$ as follows:

$$\underbrace{\begin{bmatrix}\mathbf{A} & \mathbf{B} & -2\mathbf{G}\end{bmatrix}}_{(L-1)\times 3}\begin{bmatrix}d_{1,1}^2\\ d_{2,1}^2\\ d_{1,1}d_{2,1}\end{bmatrix}+\mathbf{V}=0, \tag{30}$$

where the jth entry in vector $\mathbf{V}$ is:

$$\begin{aligned}
\mathbf{V}_j=&\,a_{j-1}\beta_j+\left(a_{j-1}-a_j\right)Y_{2,j}^2+b_{j-1}\alpha_j+\left(b_{j-1}-b_j\right)Y_{1,j}^2\\
&-2\left(c_{j-1}\gamma_j+\left(c_{j-1}-c_j\right)Y_{1,j}Y_{2,j}\right),
\end{aligned}$$

and

$$\begin{cases}\mathbf{A} &= \begin{bmatrix}\alpha_1 & \alpha_2 & \dots & \alpha_L\end{bmatrix}^T\\ \mathbf{B} &= \begin{bmatrix}\beta_1 & \beta_2 & \dots & \beta_L\end{bmatrix}^T\\ \mathbf{G} &= \begin{bmatrix}\gamma_1 & \gamma_2 & \dots & \gamma_L\end{bmatrix}^T.\end{cases}$$

The system in (30) can be solved exactly when the matrix $\begin{bmatrix}\mathbf{A} & \mathbf{B} & -2\mathbf{G}\end{bmatrix}$ has rank 3. This requires that the number of lines satisfies $L\geq 4$ [4]. Nevertheless, the problem can also be solved when $K=2$ and $L=3$, in which case we can find two solutions as described in Appendix C-B.

Then, for $L\geq 4$, we can solve (30) to uniquely retrieve $d_{1,1}^2$, $d_{2,1}^2$ and $d_{1,1}d_{2,1}$. We can then obtain $d_{1,j}^2$, $d_{2,j}^2$ and $d_{1,j}d_{2,j}$ from (28).

From the estimated parameters $d_{1,j}^2$, $d_{2,j}^2$ and $d_{1,j}d_{2,j}$, we can retrieve two different solutions for each line j, given by $\{s_jd_{1,j},\, s_jd_{2,j}\}$ for $s_j\in\{-1,1\}$.

We can then arbitrarily select the sign for the first line, and for simplicity we choose $s_1=1$. Given $d_{1,1}$ and $d_{2,1}$ we can then use Eq. (23) to infer the correct sign s_j for all subsequent lines $j=2,...,L$.

2) Estimation of the first two lines of the trajectory

Once the shortest distances from all sources to all lines have been estimated, we arbitrarily select the first line, and for simplicity we set $\mathbf{b_1}=[0,0]$, $\mathbf{c_1}=[1,0]$ and $\tilde{\mathbf{c}}_\mathbf{1}=[0,1]$. We then estimate the direction vector $\mathbf{c_2}$ of the second line from the system of equations in (22).

[4]Matrix $\begin{bmatrix}\mathbf{A} & \mathbf{B} & -2\mathbf{G}\end{bmatrix}$ may lose rank when the equations in (29) are equivalent using the parameters $Y_{k,j}$ for different lines j. This may happen for a degenerate arrangement of the sources relative to the lines in the trajectory. For example, when the lines $j-1$ and j are orthogonal, the sources $\mathbf{S_1}$ and $\mathbf{S_2}$ are collinear with the point $\mathbf{b_j}$ and the angle between $\mathbf{S_1}-\mathbf{b_j}$ and line j measures $45°$. In this case $Y_{k,j-1}-l_{j-1}=Y_{k,j}$, for $k=1,2$ and hence the jth row of matrix $\begin{bmatrix}\mathbf{A} & \mathbf{B} & -2\mathbf{G}\end{bmatrix}$ is zero.

3) Estimation of the locations of the sources

Using the estimated $\mathbf{c_2}$ and $X=\mathbf{c_1}^T\mathbf{c_2}$, we can then retrieve the location of each source k, by solving the following system of equations:

$$\begin{bmatrix}\mathbf{c_1}^T\\ \mathbf{c_2}^T\end{bmatrix}\begin{bmatrix}\mathbf{S_k}-\mathbf{b_1}\end{bmatrix}=\begin{bmatrix}Y_{k,1}\\ Y_{k,2}+l_1X\end{bmatrix}, \tag{31}$$

from which we find $\mathbf{S_k}-\mathbf{b_1}$, and hence $\mathbf{S_k}$.

4) Estimation of the amplitudes of the sources

For each source k, once we find its location $\mathbf{S_k}$, we can also find the distance from this source to the first line using $d_{k,1}^2=||\mathbf{S_1}-\mathbf{b_1}||^2-Y_{k,1}^2$, since the parameters $Y_{k,1}$ are known. Finally, we can use the parameters $A_{k,1}$ estimated using FRI, to get the amplitude of the source as $a_k=A_{k,1}e^{d_{k,1}^2}$.

5) Estimation of the remaining lines

Once the locations of two sources have been estimated, we can sequentially retrieve the parameter $\mathbf{c_j}$ of each line j from the system of equations:

$$\begin{bmatrix}\left(\mathbf{S_1}-\mathbf{b_j}\right)^T\\ \vdots\\ \left(\mathbf{S_K}-\mathbf{b_j}\right)^T\end{bmatrix}\begin{bmatrix}\mathbf{c_j}\end{bmatrix}=\begin{bmatrix}Y_{1,j}\\ \vdots\\ Y_{K,j}\end{bmatrix},$$

for $j=3,...,L$, and where $\mathbf{b_{j-1}}$ has been estimated using $\mathbf{b_j}=\mathbf{b_{j-1}}+l_j\mathbf{c_{j-1}}$.

Finally, in Appendix F we show that this solution is up to an orthogonal transformation.

B. D-SLAM when $K=2$ and $L=3$

When $K=2$ and $L=3$, matrix $\begin{bmatrix}\mathbf{A} & \mathbf{B} & -2\mathbf{G}\end{bmatrix}$ in (30) does not have full rank. Hence, we cannot uniquely find the distances $d_{k,j}$. Nevertheless, we can define:

$$\begin{aligned}
\mathbf{D_j}&=\begin{bmatrix}d_{1,j}\\ d_{2,j}\end{bmatrix}\begin{bmatrix}d_{1,j} & d_{2,j}\end{bmatrix}=\begin{bmatrix}d_{1,j}^2 & d_{1,j}d_{2,j}\\ d_{1,j}d_{2,j} & d_{2,j}^2\end{bmatrix}\\
&\overset{(a)}{=}\begin{bmatrix}d_{1,1}^2 & d_{1,1}d_{2,1}\\ d_{1,1}d_{2,1} & d_{2,1}^2\end{bmatrix}+\begin{bmatrix}a_j & c_j\\ c_j & b_j\end{bmatrix},
\end{aligned}$$

where (a) follows from (28).

Matrix $\mathbf{D_j}$ satisfies $\det\left(\mathbf{D_j}\right)=0$ and this allows us to obtain the following system of equations for $j=2,3$:

$$\begin{cases}b_2d_{1,1}^2+a_2d_{2,1}^2-2c_2d_{1,1}d_{2,1}+c_2^2-a_2b_2=0\\ b_3d_{1,1}^2+a_3d_{2,1}^2-2c_3d_{1,1}d_{2,1}+c_3^2-a_3b_3=0.\end{cases}$$

We can then set $d_{2,1}=ad_{1,1}$ to get:

$$\begin{cases}d_{1,1}^2\left(b_2+a_2a^2-2c_2a\right)+c_2^2-a_2b_2=0\\ d_{1,1}^2\left(b_3+a_3a^2-2c_3a\right)+c_3^2-a_3b_3=0.\end{cases}$$

Equating the two expressions for $d_{1,1}^2$ we have that:

$$\begin{aligned}
&\left(c_3^2-a_3b_3\right)\left(b_2+a_2a^2-2c_2a\right)=\\
&\qquad\left(c_2^2-a_2b_2\right)\left(b_3+a_3a^2-2c_3a\right),
\end{aligned}$$

which we can solve to retrieve two values for the unknown a.

Therefore, there are two solutions for $d_{1,1}^2$ and hence two solutions for the source locations and trajectory. However, at least one of these solutions ensures the estimated inner products between vectors are equal to the true inner product

values (i.e. the parameter $X = \mathbf{c_1}^T\mathbf{c_2}$ is correctly retrieved in one of these solutions, given the estimation is based on ideal parameters $Y_{k,j}$). As a result, this solution will be consistent with the field measurements and up to an orthogonal transformation from the true source locations and trajectory, as shown in Appendix F.

APPENDIX D
D-SLAM FOR ONE SOURCE AND CLOSED TRAJECTORY

When $K = 1$, the only knowledge we have is $\mathbf{c_j}\left(\mathbf{S_1} - \mathbf{b_j}\right) = Y_{1,j}$ for $j = 1, ..., L$ and hence, it is not possible to use the method in Appendix C to estimate the source location $\mathbf{S_1}$ and the piecewise linear trajectory. Nevertheless, by leveraging the fact that the lines in the trajectory belong to a 2D plane and by assuming the trajectory is closed (such that the end point coincides with the start of the trajectory), we can solve the problem as follows.

For simplicity, let us consider the case in which the trajectory is closed and composed of $L = 3$ lines. We denote the term $\mathbf{c_1}^T\mathbf{c_2} = X$, and try to express the parameters $Y_{k,j}$ we estimate for each source k and line j, as a function of the unknown X. We can replace $\mathbf{b_2} = \mathbf{b_1} + l_1\mathbf{c_1}$ and $\mathbf{b_3} = \mathbf{b_2} + l_2\mathbf{c_2} = \mathbf{b_1} + l_1\mathbf{c_1} + l_2\mathbf{c_2}$ in Eq. (4), to get:

$$\begin{cases} \mathbf{c_1}^T(\mathbf{S_1} - \mathbf{b_1}) = Y_{1,1} \\ \mathbf{c_2}^T(\mathbf{S_1} - \mathbf{b_1} - l_1\mathbf{c_1}) = Y_{1,2} \\ \mathbf{c_3}^T(\mathbf{S_1} - \mathbf{b_1} - l_1\mathbf{c_1} - l_2\mathbf{c_2}) = Y_{1,3}, \end{cases}$$

which we can re-write as:

$$\begin{cases} \mathbf{c_1}^T(\mathbf{S_1} - \mathbf{b_1}) = Y_{1,1} \\ \mathbf{c_2}^T(\mathbf{S_1} - \mathbf{b_1}) = Y_{1,2} + l_1\mathbf{c_1}^T\mathbf{c_2} \\ \mathbf{c_3}^T(\mathbf{S_1} - \mathbf{b_1}) = Y_{1,3} + l_1\mathbf{c_3}^T\mathbf{c_1} + l_2\mathbf{c_3}^T\mathbf{c_2} \end{cases}$$

or equivalently, in matrix form:

$$\begin{bmatrix} \mathbf{c}_1^T \\ \mathbf{c}_2^T \\ \mathbf{c}_3^T \end{bmatrix} \left[\mathbf{S_1} - \mathbf{b_1}\right] = \begin{bmatrix} Y_{1,1} \\ Y_{1,2} + l_1\mathbf{c_1}^T\mathbf{c_2} \\ Y_{1,3} + l_1\mathbf{c_3}^T\mathbf{c_1} + l_2\mathbf{c_3}^T\mathbf{c_2} \end{bmatrix}. \quad (32)$$

Since we are considering a diffusion problem in 2D, we have $\mathbf{c_j} \in \mathbb{R}_2$. This means that we can find α and β such that $\mathbf{c_3} = \alpha\mathbf{c_1} + \beta\mathbf{c_2}$. As a result, we get $\mathbf{c_3}^T\mathbf{c_1} = \alpha\mathbf{c_1}^T\mathbf{c_1} + \beta\mathbf{c_2}^T\mathbf{c_1}$, which knowing $\mathbf{c_1}^T\mathbf{c_1} = \mathbf{c_2}^T\mathbf{c_2} = 1$ and $\mathbf{c_1}^T\mathbf{c_2} = X$, can be re-written as $\mathbf{c_3}^T\mathbf{c_1} = \alpha + \beta X$. Similarly, $\mathbf{c_3}^T\mathbf{c_2} = \alpha X + \beta$. Then, we can re-write Eq. (32) as:

$$\underbrace{\begin{bmatrix} \mathbf{c}_1^T \\ \mathbf{c}_2^T \\ \mathbf{c}_3^T \end{bmatrix}}_{\mathbf{C}} \left[\mathbf{S_1} - \mathbf{b_1}\right] = \underbrace{\begin{bmatrix} Y_{1,1} \\ Y_{1,2} + l_1 X \\ Y_{1,3} + l_1(\alpha + \beta X) + l_2(\alpha X + \beta) \end{bmatrix}}_{\mathbf{d}}.$$

We know that this system of equations must have at least one solution, due to the physics of the problem. Moreover, provided none of the three lines are parallel, then $\mathrm{rank}\,(\mathbf{C}) = 2$. Given the system above is an overdetermined system with 3 equations and 2 unknowns, $\mathrm{rank}\,(\mathbf{C}) = 2$ implies that this solution is unique. In addition, in order for this solution to exist, we must also have that $\mathrm{rank}\left(\mathbf{C}|\mathbf{d}\right) = \mathrm{rank}\,(\mathbf{C}) = 2$. In order to ensure $\mathrm{rank}\left(\mathbf{C}|\mathbf{d}\right) = 2$ we then need to impose:

$$Y_{1,3} + l_1(\alpha + \beta X) + l_2(\alpha X + \beta) = \alpha Y_{1,1} + \beta(Y_{1,2} + l_1 X),$$

or equivalently:

$$\alpha(l_1 + l_2 X - Y_{1,1}) + \beta(l_2 - Y_{1,2}) + Y_{1,3} = 0. \quad (33)$$

Given the trajectory is closed, we have $\mathbf{c_3} = -\mathbf{c_1} - \mathbf{c_2}$, which means that $\alpha = \beta = -1$. We can then replace these values in (33), in order to obtain $X = \mathbf{c_1}^T\mathbf{c_2}$. Finally, we can retrieve the location of the source as in Eq. (31).

APPENDIX E
D-SLAM IN 3D

In a *d*-dimentional space,where $d \geq 1$, the Green's function for the diffusion field becomes [5]:

$$f(\mathbf{x}, t) = \frac{1}{\left(4\pi\mu(t - \tau_k)\right)^{\frac{d}{2}}} a_k e^{-\frac{||\mathbf{x} - \mathbf{S_k}||^2}{4\mu(t-\tau_k)}} H(t - \tau_k),$$

where $d = 3$ for propagation in a 3D space.

Following the derivations in Section II, at discrete uniform points $\mathbf{q_j}(nT_s)$ along line j, the diffusion field for $d = 3$ is:

$$f(\mathbf{q_{j,n}}) = f_j(nT_s) = \sum_{k=1}^{K} \bar{A}_{k,j} e^{-\frac{(l_j nT_s - Y_{k,j})^2}{C_k(t)}},$$

where $C_k(t) = 4\mu\,(t - \tau_k)$ and:

$$\bar{A}_{k,j} = \frac{a_k}{\left(\pi C_k(t)\right)^{\frac{3}{2}}} e^{-\frac{||\mathbf{b_j} - \mathbf{S_k}||^2 - \left((\mathbf{b_j} - \mathbf{S_k})^T\mathbf{c_j}\right)^2}{C_k(t)}},$$

$$Y_{k,j} = \left(\mathbf{S_k} - \mathbf{b_j}\right)^T \mathbf{c_j}.$$

We can then use the derivations in Section III, to retrieve the parameters $\bar{A}_{k,j}$ and $Y_{k,j}$. The only difference is that, given we are now in a 3D space, matrix $\mathbf{A}$ in (14) will be a symmetric 3×3 matrix, with 6 unknowns. As a result, we need $L \geq 6$ lines in order to estimate these unknowns. In addition, the factorisation in (13) requires $\mathrm{rank}\,(\Omega) = 3$, which is the case for $K \geq 4$ sources not located in the same plane.

In summary, if we allow the diffusion field to propagate in a 3D space, we can estimate the sources and trajectory up to an orthogonal transformation, provided $K \geq 4$ and $L \geq 6$.

APPENDIX F
D-SLAM SOLUTION IS UP TO AN ORTHOGONAL TRANSFORMATION

In Appendix C we have presented sufficient conditions that ensure we retrieve a unique solution for $K = 2$ and $L \geq 4$. In what follows, we show that this will be up to an orthogonal transformation from the true source locations and trajectory (i.e. the inner products between vectors are preserved).

Let us denote the true direction vectors with $\mathbf{c_j}$ and the estimated ones with $\tilde{\mathbf{c}}_\mathbf{j}$. Similarly, we denote the true source locations with $\mathbf{S_k}$ and the estimated locations with $\tilde{\mathbf{S}}_\mathbf{k}$. As we have seen in Appendix C-A2, we can exactly retrieve $\mathbf{c_1}^T\mathbf{c_2}$ from the parameters $Y_{k,j}$. This ensures:

$$\mathbf{c_1}^T\mathbf{c_2} = \tilde{\mathbf{c}}_\mathbf{1}^T\tilde{\mathbf{c}}_\mathbf{2}. \quad (34)$$

Suppose $\mathbf{c_1} = \mathbf{Q}\tilde{\mathbf{c}}_\mathbf{1}$. Then, given ${\mathbf{c_1}}^T\mathbf{c_1} = 1$, we get $\tilde{\mathbf{c}}_\mathbf{1}^T\mathbf{Q}^T\mathbf{Q}\tilde{\mathbf{c}}_\mathbf{1} = 1$. Moreover, since $\tilde{\mathbf{c}}_\mathbf{1}$ also satisfies $\tilde{\mathbf{c}}_\mathbf{1}^T\tilde{\mathbf{c}}_\mathbf{1} = 1$, this shows that $\mathbf{Q}^T\mathbf{Q} = \mathbf{I}$, i.e. that $\mathbf{Q}$ is orthogonal. Then, from $\tilde{\mathbf{c}}_\mathbf{1}^T\tilde{\mathbf{c}}_\mathbf{2} = {\mathbf{c_1}}^T\mathbf{c_2}$ in Eq. (34), we get $\tilde{\mathbf{c}}_\mathbf{1}^T\tilde{\mathbf{c}}_\mathbf{2} = \tilde{\mathbf{c}}_\mathbf{1}^T\mathbf{Q}^T\mathbf{c_2}$, which gives $\tilde{\mathbf{c}}_\mathbf{2} = \mathbf{Q}^T\mathbf{c_2}$, or equivalently $\mathbf{c_2} = \mathbf{Q}\tilde{\mathbf{c}}_\mathbf{2}$.

In addition, we have seen that we can then retrieve the sources from the equation:

$$\begin{bmatrix}\tilde{\mathbf{c}}_1^T\\ \tilde{\mathbf{c}}_2^T\end{bmatrix}\left[\tilde{\mathbf{S}}_\mathbf{k} - \tilde{\mathbf{b}}_\mathbf{1}\right] = \begin{bmatrix}Y_{k,1}\\ Y_{k,2} + \tilde{\mathbf{c}}_\mathbf{1}^T\tilde{\mathbf{c}}_\mathbf{2},\end{bmatrix}$$

where we can replace $\tilde{\mathbf{c}}_\mathbf{1}^T\tilde{\mathbf{c}}_\mathbf{2} = {\mathbf{c_1}}^T\mathbf{c_2}$, to get:

$$\begin{aligned}\begin{bmatrix}\tilde{\mathbf{c}}_1^T\\ \tilde{\mathbf{c}}_2^T\end{bmatrix}\left[\tilde{\mathbf{S}}_\mathbf{k} - \tilde{\mathbf{b}}_\mathbf{1}\right] &= \begin{bmatrix}Y_{k,1}\\ Y_{k,2} + \tilde{\mathbf{c}}_\mathbf{1}^T\tilde{\mathbf{c}}_\mathbf{2}\end{bmatrix} = \begin{bmatrix}Y_{k,1}\\ Y_{k,2} + {\mathbf{c_1}}^T\mathbf{c_2}\end{bmatrix}\\ &= \begin{bmatrix}{\mathbf{c_1}}^T\\ {\mathbf{c_2}}^T\end{bmatrix}\left[\mathbf{S_k} - \mathbf{b_1}\right].\end{aligned} \tag{35}$$

Since $\tilde{\mathbf{c}}_\mathbf{1} = \mathbf{Q}\mathbf{c_1}$, $\tilde{\mathbf{c}}_\mathbf{2} = \mathbf{Q}\mathbf{c_2}$ and $\mathbf{Q}^T\mathbf{Q} = \mathbf{I}$, from Eq. (35) we get $\mathbf{S_k} - \mathbf{b_1} = \mathbf{Q}(\tilde{\mathbf{S}}_\mathbf{k} - \tilde{\mathbf{b}}_\mathbf{1})$. As a result, we also have that $\tilde{\mathbf{S}}_\mathbf{k} = \mathbf{Q}^T\mathbf{S_k}$, showing that the estimated source locations are also up to an orthogonal transformation from the true locations.

REFERENCES

[1] R. Alexandru, T. Blu, and P. L. Dragotti. D-SLAM: Diffusion Source Localization and Trajectory Mapping. In *ICASSP 2020 - 2020 IEEE International Conference on Acoustics, Speech and Signal Processing (ICASSP)*, pages 5600–5604, 2020.

[2] I. Dokmanic, J. Ranieri, A. Chebira, and M. Vetterli. Sensor networks for diffusion fields: Detection of sources in space and time. In *2011 49th Annual Allerton Conference on Communication, Control, and Computing (Allerton)*, pages 1552–1558, 2011.

[3] J. Murray-Bruce and P. L. Dragotti. Estimating Localized Sources of Diffusion Fields Using Spatiotemporal Sensor Measurements. *IEEE Transactions on Signal Processing*, 63:3018–3031, Jun 2015.

[4] J. Murray-Bruce and P. L. Dragotti. Physics-driven quantized consensus for distributed diffusion source estimation using sensor networks. *EURASIP Journal on Advances in Signal Processing*, 2016:14, 2016.

[5] J. Murray-Bruce and P. L. Dragotti. A Sampling Framework for Solving Physics-Driven Inverse Source Problems. *IEEE Transactions on Signal Processing*, 65(24):6365–6380, Dec 2017.

[6] J. Ranieri, I. Dokmanic, A. Chebira, and M. Vetterli. Sampling and reconstruction of time-varying atmospheric emissions. In *2012 IEEE International Conference on Acoustics, Speech and Signal Processing (ICASSP)*, pages 3673–3676, 2012.

[7] Y. M. Lu, P. L. Dragotti, and M. Vetterli. Localizing point sources in diffusion fields from spatiotemporal measurements. In *Proc. Int. Conf. Sampling Theory and applications (SampTA)*, Singapore, 2011.

[8] J. Ranieri, A. Chebira, Y. M. Lu, and M. Vetterli. Sampling and reconstructing diffusion fields with localized sources. In *2011 IEEE International Conference on Acoustics, Speech and Signal Processing (ICASSP)*, pages 4016–4019, May 2011.

[9] A. Flinth and A. Hashemi. Approximate recovery of initial point-like and instantaneous sources from coarsely sampled thermal fields via infinite-dimensional compressed sensing. In *2018 26th European Signal Processing Conference (EUSIPCO)*, pages 1720–1724, Sep. 2018.

[10] A. Nehorai, B. Porat, and E. Paldi. Detection and localization of vapor-emitting sources. *IEEE Transactions on Signal Processing*, 43(1):243–253, 1995.

[11] H. Paul and R. Jedermann. Sparse point source estimation in sensor networks with gaussian kernels. In *WSA 2016; 20th International ITG Workshop on Smart Antennas*, pages 1–7, 2016.

[12] M. Ortner and A. Nehorai. A sequential detector for biochemical release in realistic environments. *IEEE Transactions on Signal Processing*, 55(8):4173–4182, 2007.

[13] M. Ortner, A. Nehorai, and A. Jeremic. Biochemical transport modeling and bayesian source estimation in realistic environments. *IEEE Transactions on Signal Processing*, 55(6):2520–2532, 2007.

[14] T. Zhao and A. Nehorai. Detecting and estimating biochemical dispersion of a moving source in a semi-infinite medium. *IEEE Transactions on Signal Processing*, 54(6):2213–2225, 2006.

[15] M. Rostami, N. Cheung, and T. Q. S. Quek. Compressed sensing of diffusion fields under heat equation constraint. In *2013 IEEE International Conference on Acoustics, Speech and Signal Processing*, pages 4271–4274, 2013.

[16] S. Salgia and A. Kumar. Bandlimited spatiotemporal field sampling with location and time unaware mobile sensors. In *2018 IEEE International Conference on Acoustics, Speech and Signal Processing, ICASSP 2018, Calgary, AB, Canada, April 15-20, 2018*, pages 4574–4578. IEEE, 2018.

[17] G. Reise, G. Matz, and K. Grochenig. Distributed field reconstruction in wireless sensor networks based on hybrid shift-invariant spaces. *IEEE Transactions on Signal Processing*, 60(10):5426–5439, 2012.

[18] T. van Waterschoot and G. Leus. Static field estimation using a wireless sensor network based on the finite element method. In *2011 4th IEEE International Workshop on Computational Advances in Multi-Sensor Adaptive Processing (CAMSAP)*, pages 369–372, 2011.

[19] T. van Waterschoot and G. Leus. Distributed estimation of static fields in wireless sensor networks using the finite element method. In *2012 IEEE International Conference on Acoustics, Speech and Signal Processing (ICASSP)*, pages 2853–2856, 2012.

[20] A. Kumar, P. Ishwar, and K. Ramchandran. High-resolution distributed sampling of bandlimited fields with low-precision sensors. *IEEE Transactions on Information Theory*, 57(1):476–492, 2011.

[21] A. Kumar. On bandlimited field estimation from samples recorded by a location-unaware mobile sensor. *IEEE Transactions on Information Theory*, 63(4):2188–2200, 2017.

[22] D. Marco, E. J. Duarte-Melo, M. Liu, and D. L. Neuhoff. On the many-to-one transport capacity of a dense wireless sensor network and the compressibility of its data. In Feng Zhao and Leonidas Guibas, editors, *Information Processing in Sensor Networks*, pages 1–16, Berlin, Heidelberg, 2003. Springer Berlin Heidelberg.

[23] S. Yan, C. Wu, W. Dai, M. Ghanem, and Y. Guo. Environmental monitoring via compressive sensing. In *Proceedings of the Sixth International Workshop on Knowledge Discovery from Sensor Data*, SensorKDD '12, page 6168, New York, NY, USA, 2012. Association for Computing Machinery.

[24] S. Kitić, L. Albera, N. Bertin, and R. Gribonval. Physics-driven inverse problems made tractable with cosparse regularization. *IEEE Transactions on Signal Processing*, 64(2):335–348, 2016.

[25] M. Chino, H. Nakayama, H. Nagai, H. Terada, G. Katata, and H. Yamazawa. Preliminary Estimation of Release Amounts of 131 I and 137 Cs Accidentally Discharged from the Fukushima Daiichi Nuclear Power Plant into the Atmosphere. 2011.

[26] J. Matthes, L. Groll, and H. B. Keller. Source localization by spatially distributed electronic noses for advection and diffusion. *IEEE Transactions on Signal Processing*, 53(5):1711–1719, 2005.

[27] A. Aldroubi, C. Cabrelli, U. Molter, and S. Tang. Dynamical sampling. *Applied and Computational Harmonic Analysis*, 42(3):378 – 401, 2017.

[28] A. Jeremic and A. Nehorai. Design of chemical sensor arrays for monitoring disposal sites on the ocean floor. In *Proceedings of the 1998 IEEE International Conference on Acoustics, Speech and Signal Processing, ICASSP '98 (Cat. No.98CH36181)*, volume 4, pages 2013–2016, 1998.

[29] B. A. Egan and J. R. Mahoney. Numerical Modeling of Advection and Diffusion of Urban Area Source Pollutants. *Journal of Applied Meteorology*, 11(2):312–322, March 1972.

[30] J. Unnikrishnan and M. Vetterli. Sampling and reconstruction of spatial fields using mobile sensors. *IEEE Transactions on Signal Processing*, 61(9):2328–2340, 2013.

[31] B. Porat and A. Nehorai. Localizing vapor-emitting sources by moving sensors. *IEEE Transactions on Signal Processing*, 44(4):1018–1021, 1996.

[32] A. Shallom, H. Kirshner, and M. Porat. Adaptive reconstruction along mobile sensing paths. In *2018 IEEE Statistical Signal Processing Workshop (SSP)*, pages 308–312, Jun 2018.

[33] A. Bahr and J. J. Leonard. *Cooperative Localization for Autonomous Underwater Vehicles*, pages 387–395. Springer Berlin Heidelberg, Berlin, Heidelberg, 2008.

[34] C. Cadena, L. Carlone, H. Carrillo, Y. Latif, D. Scaramuzza, J. Neira, I. Reid, and J.J. Leonard. Past, present, and future of simultaneous localization and mapping: Towards the robust-perception age. *IEEE Transactions on Robotics*, 32(6):13091332, 2016.

[35] H. Durrant-Whyte and T. Bailey. Simultaneous localization and mapping: part I. *IEEE Robotics Automation Magazine*, 13(2):99–110, 2006.

[36] A. J. Davison, I. D. Reid, N. D. Molton, and O. Stasse. MonoSLAM: Real-Time Single Camera SLAM. *IEEE Transactions on Pattern Analysis and Machine Intelligence*, 29(6):1052–1067, 2007.

[37] C. Evers and P. A. Naylor. Acoustic SLAM. *IEEE/ACM Transactions on Audio, Speech, and Language Processing*, 26(9):1484–1498, 2018.

[38] I. Dokmanic and L. Daudet and M. Vetterli. From acoustic room reconstruction to SLAM. In *2016 IEEE International Conference on Acoustics, Speech and Signal Processing (ICASSP)*, pages 6345–6349, 2016.

[39] R. Guo and T. Blu. FRI Sensing: Sampling Images along Unknown Curves. In *ICASSP 2019 - 2019 IEEE International Conference on Acoustics, Speech and Signal Processing (ICASSP)*, pages 5132–5136, May 2019.

[40] R. Guo and T. Blu. FRI Sensing: Retrieving the Trajectory of a Mobile Sensor From Its Temporal Samples. *IEEE Transactions on Signal Processing*, 68:5533–5545, 2020.

[41] M. A. Adegboye, W.-K. Fung, and A. K. Recent advances in pipeline monitoring and oil leakage detection technologies: Principles and approaches. *Sensors*, 19(11), 2019.

[42] Deepak Aeloor and Neeta Patil. A survey on odour detection sensors. In *2017 International Conference on Inventive Systems and Control (ICISC)*, pages 1–5, 2017.

[43] K. Watanabe. *Integral Transform Techniques for Green's Function by Kazumi Watanabe.* Lecture Notes in Applied and Computational Mechanics, 71. Springer International Publishing, Cham, i1st ed. 2014. edition, 2014.

[44] M. Vetterli, P. Marziliano, and T. Blu. Sampling signals with finite rate of innovation. *IEEE Transactions on Signal Processing*, 50(6):1417–1428, Jun 2002.

[45] T. Blu, P. Dragotti, M. Vetterli, P. Marziliano, and L. Coulot. Sparse sampling of signal innovations. *IEEE Signal Processing Magazine*, 25(2):31–40, Mar 2008.

[46] T. Blu R. Alexandru and P. L. Dragotti. Localising diffusion sources from samples taken along unknown parametric trajectories. In *2021 29th European Signal Processing Conference (EUSIPCO)*, Sep. 2021.

[47] M. Pacholska, F. Dümbgen, and A. Scholefield. Relax and recover: Guaranteed range-only continuous localization. *IEEE Robotics and Automation Letters*, 5(2):2248–2255, 2020.

[48] Y. Hua and T. K. Sarkar. Matrix pencil method for estimating parameters of exponentially damped/undamped sinusoids in noise. *IEEE Transactions on Acoustics, Speech, and Signal Processing*, 38(5):814–824, 1990.

[49] B. D. Rao and K. S. Arun. Model based processing of signals: a state space approach. *Proceedings of the IEEE*, 80(2):283–309, 1992.

[50] I. Maravic and M. Vetterli. Sampling and reconstruction of signals with finite rate of innovation in the presence of noise. *IEEE Transactions on Signal Processing*, 53(8):2788–2805, 2005.

[51] C. Gilliam and T. Blu. Finding the minimum rate of innovation in the presence of noise. In *2016 IEEE International Conference on Acoustics, Speech and Signal Processing (ICASSP)*, pages 4019–4023, 2016.

[52] P. Stoica and R. Moses. *Spectral Analysis of Signals*. 2005.

[53] J. A. Urigüen, T. Blu, and P. L. Dragotti. FRI Sampling With Arbitrary Kernels. *IEEE Transactions on Signal Processing*, 61(21):5310–5323, Nov 2013.

[54] R. Prony. Essai expérimental et analytique sur les lois de la dilatabilité de fluides élastiques et sur celles de la force expansive de la vapeur de l'eau et de la vapeur de l'alkool, à différentes températures. *Journal de l'École Polytechnique*, 1(22):24–76.

[55] P. L. Dragotti, M. Vetterli, and T. Blu. Sampling Moments and Reconstructing Signals of Finite Rate of Innovation: Shannon Meets Strang-Fix. *IEEE Transactions on Signal Processing*, 55(5):1741–1757, May 2007.